

Function of the Mammalian Postorbital Bar

Christopher P. Heesy*

Department of Anatomy, New York College of Osteopathic Medicine, Old Westbury, New York 11568

ABSTRACT Complete postorbital bars, bony arches that encompass the lateral aspect of the eye and form part of a circular orbit, have evolved homoplastically multiple times during mammalian evolution. Numerous functional hypotheses have been advanced for postorbital bars, the most promising being that postorbital bars function to stiffen the lateral orbit in taxa that have significant angular deviation between the temporal fossa and the bony orbit. Without a stiff lateral orbit the anterior temporalis muscle and fascia potentially would pull on the postorbital ligament, deform the orbit, and cause disruption of oculomotor precision. Morphometric data were collected on 1,329 specimens of 324 taxa from 16 orders of extant eutherian and metatherian mammals in order to test whether the orientation of the orbit relative to the temporal fossa is correlated with the replacement of the postorbital ligament with bone. The allometric and ecological influences on orbit orientation across mammals are also explored. The morphometric results corroborate the hypothesis: Shifts in orbit orientation relative to the temporal fossa are correlated with the size of the postorbital processes, which replace the ligament. The allometric and ecological factors that influence orbit orientation vary across taxa. Postorbital bars stiffen the lateral orbital wall. Muscle pulleys, ligaments, and other connective tissue attach to the lateral orbital wall, including the postorbital bar. Without a stiff lateral orbit, deformation due to temporalis contraction would displace soft tissues contributing to normal oculomotor function. *J. Morphol.* 264: 363–380, 2005. © 2005 Wiley-Liss, Inc.

KEY WORDS: orbit orientation; binocular vision; stereopsis; diplopia; mastication; mammals

Complete postorbital bars, bony arches that encompass the lateral aspect of the eye and form part of a circular orbit, have evolved at least 11 times in nine mammalian orders and are characteristic of Primates, Scandentia, Equinae (Equidae, Perissodactyla), and the Neoselenodontia (Artiodactyla). Postorbital bars are commonly formed by a dorsal process of the frontal bone and a ventral process of the zygomatic (Heesy, 2003). Equines differ in that the squamosal projects the ventral process (Heesy, 2003). Postorbital bars have also evolved independently in numerous individual taxa including the fossil metatherians *Thylacosmilus* and *Thylacoleo*, the fossil carnivoran *Barbourofelis*, the fossil liopterns *Thoatherium* and *Diadiaphorus*, the sirenian *Trichechus senegalensis*, and the mysticete cetacean *Bala-*

noptera acutorostrata. Well-developed postorbital processes, the probable intermediate condition from which postorbital bars are derived, have evolved in dermopterans, emballonurid microchiropterans, pteropodid megachiropterans, hyracoids, and, to varying degrees, among many carnivoran taxa. Polymorphisms of well-developed postorbital processes (retaining a small gap of several millimeters that would be spanned by the postorbital ligament in life) and complete bars are also found in a number of small-bodied pteropodid, carnivoran, and hyracoid taxa (Cartmill, 1970; Noble et al., 2000; Ravosa et al., 2000b; Heesy, 2003).

Numerous functional hypotheses have been advanced for postorbital bars (reviewed in Heesy, 2003). Three of these are commonly cited. For example, Prince (1953, 1956) and Simons (1962) hypothesized that postorbital closure (including the possession of postorbital bars) functions to protect the lateral aspect of the orbital contents from external trauma. Cartmill (1970) pointed out that the bar would be inadequate to protect the orbital contents in strepsirrhine primates from a sharp attack, such as a tooth, because the bar is slender and thus fails to cover much of the lateral orbital wall. An intrusion from the lateral side would be more likely to pierce the eye than contact such a slender structure as is found in strepsirrhine primates, tree shrews, and herpestids, and would therefore likely be inadequate to protect the eye from such attacks.

Greaves (1985) suggested that the function of the postorbital bar in primates and ungulates was related to mastication. Greaves (1985) hypothesized that the application of a unilateral bite force on the rostrum, the application of a contralateral condylar

This article includes Supplementary Material available via the internet at <http://www.interscience.wiley.com/jpages/0362-2525/suppmat>

Contract grant sponsor: the Leakey Foundation.

*Correspondence to: Christopher Paul Heesy, New York College of Osteopathic Medicine, Department of Anatomy, Riland Bldg., Room 321, Old Westbury, NY 11568. E-mail: cheesy@nyit.edu

Published online 20 April 2005 in
Wiley InterScience (www.interscience.wiley.com)
DOI: 10.1002/jmor.10334

joint reaction force on the braincase, and the bilateral muscle forces due to the contraction of the masticatory musculature apply torsional moments to the mammalian skull. Greaves further hypothesized that shear stress due to torsional loading would be most extreme in taxa with large and dominant masseter and medial pterygoid muscles because of the significantly larger moment arms of these muscles compared to those of the temporalis muscles. Pronounced postorbital constriction would also lower resistance to torsional stresses because this resistance is related to the distribution of mass away from the axis of twisting. The presence of postorbital bars in primates and neoselenodonts led Greaves to hypothesize that this structure functions to reinforce the structurally weak postorbital region against torsional loading. However, the postorbital bars and septa in primates are not oriented along Greaves' helices of tension and compression (Ravosa, 1991a,b), and the strain orientations in the circumorbital region of anthropoids do not support a torsional loading regime (Hylander et al., 1991; Ross and Hylander, 1996). Although strain orientations in galagos do match the predictions of Greaves' hypothesis, the strain magnitudes are likely too low to require the presence of postorbital bars to prevent craniofacial torsion in masticating strepsirrhines (Ravosa et al., 2000a; Ross, 2001). The "weak" postorbital region also does not experience substantially higher strain magnitudes during loading when the postorbital bars are removed in *Ovis* (Heesy et al., unpubl. in vitro strain data).

An alternative hypothesis has been suggested based on the position of the orbit relative to the temporal fossa in mammals. Cartmill (1970, 1972, 1980; see also Collins, 1921) suggested that in small-sized therian mammals with large eyes, relatively small temporal fossae, and derived orbital convergence (orbits facing in the same direction), the plane of the bony orbit would deviate from the "plane" of the temporal fossa. Cartmill proposed that increasing orbital convergence "drags" the anterior temporalis muscle and temporalis fascia from a posterior to a lateral position relative to the fundus of the eye and orbital contents (Fig. 1). In such taxa, Cartmill suggested that contractions of the masticatory musculature, particularly the anterior temporalis muscle, would be likely to distort the lateral orbital margin, which is formed by the postorbital ligament. The postorbital ligament is a thickening of the anteriormost edge of the temporalis fascia (Hiimae and Jenkins, 1969; Cartmill, 1970), and contraction of the anterior temporalis muscle would create tension across the fascial sheet, including the ligament, and cause the tensed ligament to be deformed medially, posteriorly, or posteromedially. Extraocular check ligaments and smooth muscle tissue attach to the lateral orbital margin that are critical for maintenance of the mediolateral rotational axis of the eye and oculomotor coordination (Demer et al., 1995,

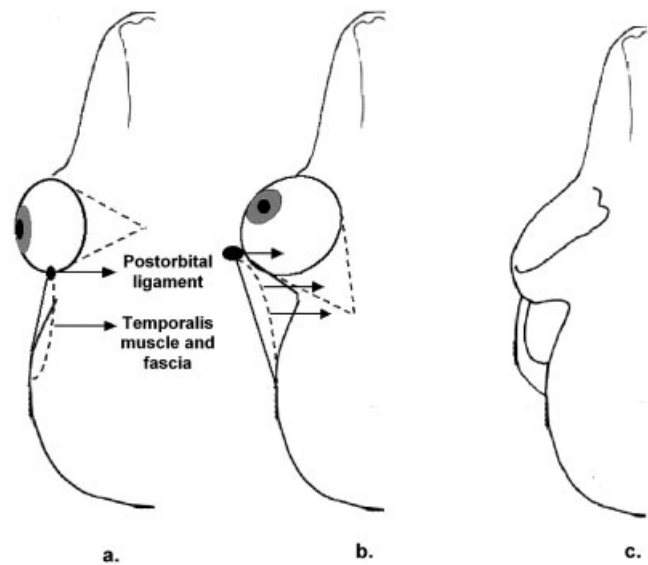


Fig. 1. Cartmill's hypothesized effects of orbit orientation on postorbital ossification. In many mammals the temporalis fascia and postorbital ligament, which is the anteriormost edge of this fascia, sit posterior to the eye (a). Cartmill hypothesized that increasing orbital convergence drags the ligament anterolaterally (b), where it can be deformed during anterior temporalis contraction and temporalis fascia tension (indicated by arrows). Preventing disruptive eye movements during mastication requires the evolution of postorbital processes or a bar to prevent the fascia from encroaching on the eye (c).

1997, 2000; Clark et al., 1997, 1998; Khanna and Porter, 2001; Briggs and Schachat, 2002; Demer, 2002; Haslwanter, 2002; Heesy et al., 2005; see Discussion). Deformation of a ligamentous lateral orbital margin would displace these attachments to the eye and probably disrupt oculomotor precision by irregularly translating the mediolateral rotational axis with each contraction of the anterior temporalis muscle. Replacement of the postorbital ligament with an osseous postorbital bar should stiffen the lateral bony orbit and, thereby, prevent oculomotor disruption. Intermediate morphology, such as large postorbital processes bridged by a taut postorbital ligament, would provide a minimally stable substrate for these check ligament attachments in taxa with intermediate degrees of orbit convergence. Examples of disruption are double vision (diplopia), image blur, and jitter due to misalignment of the optic and visual axes, which in humans causes visual confusion and vertigo (see Heesy, 2003; Heesy et al., 2005).

Cartmill's hypothesis predicts that increasing the angular or planar deviation between the orbit and the temporalis fascia should lead to increased replacement of the postorbital ligament with postorbital processes and other stiffening structures in order to prevent disruption of oculomotor coordination. Cartmill also predicted that relative orbit size is a factor in reorienting the orbit away from the temporal fossa. Taxa such as megachiropterans and

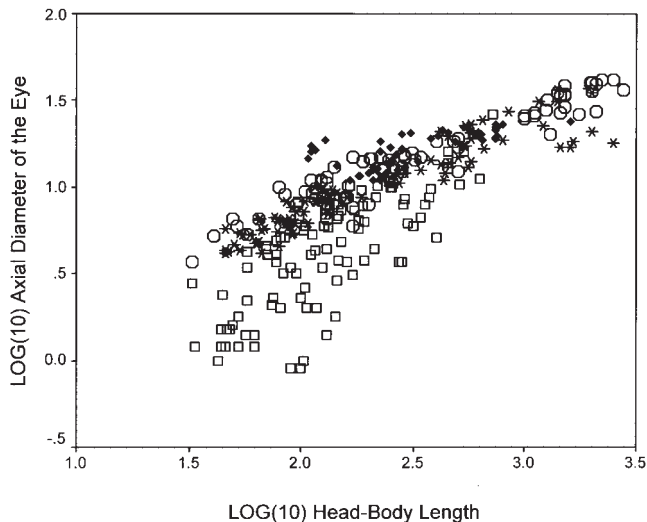


Fig. 2. Eye size and the morphology of the posterolateral orbital wall. When the axial length of the eye is plotted against head-body length (both Log_{10}), it is shown that taxa with large processes, or bars, tend to have larger eye sizes than taxa without processes. Haplorhine primates (tarsiers, monkeys, apes, and humans) have postorbital septa, bony walls that largely wall off the lateral orbit from the temporal fossa. (Data on eye and body size from Ritland, 1982, and Ross et al., 2005. Data on postorbital morphology are available as Supplementary Material at www.interscience.wiley.com/jpages/0362-2525/suppmat.) \square , no/small postorbital process; $*$, process; \circ , bar; \blacklozenge , septum.

small-bodied herpestid carnivorans with slightly lesser degrees of orbital convergence than most strepsirrhines (Cartmill, 1970) have well-developed postorbital processes, corroborating Cartmill's hypothesis (Noble et al., 2000; Ravosa et al., 2000b). Ravosa and colleagues (Noble et al., 2000; Ravosa et al., 2000a), in an analysis of megachiropterans and herpestid and felid carnivorans, found that frontation (vertical orbit orientation relative to the long axis of the braincase) as well as relative encephalization and orbit:body size allometry (a factor identified by Cartmill) are contributing factors to the evolution of bars among these taxa. The association between bone strain patterns and anterior temporalis contraction has not been directly evaluated. However, *in vivo* bone strain data collected on the lateral aspect of the postorbital bar of the strepsirrhine primate *Otolemur* indicate that it experiences nontrivial levels of strain during mastication (Ravosa et al., 2000a,b). This suggests that if a postorbital ligament was in place of the bar, the lateral orbit would be deformed by temporalis contraction. Lastly, mammals with large eye sizes relative to body size tend to have postorbital processes or bars (Fig. 2).

While Cartmill's hypothesis potentially explains the presence of postorbital bars in small-sized taxa with convergent orbits, it is not completely explanatory for all mammals with postorbital bars because it does not explain their presence in groups with

laterally directed orbits: neoselenodont artiodactyls, equine perissodactyls, and scandentians. It is suggested here, however, that convergence is not the only type of orbit reorientation that would lead to a substantial angular deviation between the orbit and temporal fossa (Fig. 3). Dissections of *Ovis*, and observations of the morphology of this group, suggest that large eye size in neoselenodonts has led to an increase in the exposure of the posterolateral aspect of the eye and orbital cone to the temporal structures and in the lateral displacement of the posterolateral orbital margin (Fig. 3a). This displacement dragged the superficial layer of the temporalis fascia laterally, which is similar to the deviation of the orbital and temporal fossa planes that Cartmill suggested would lead to distortions of the orbital margin in taxa with convergent orbits. In other words, the lateral displacement of the posterior orbital margin in neoselenodonts may have decreased the medial angle between the orbital and temporal planes, thereby resulting in a spatially constrained posterolateral orbital region similar to that in taxa with convergent orbits. The displacement and reorientation of the orbit during equid evolution may have had a similar effect in this group (Radinsky, 1983, 1984) (Fig. 3b). In addition, one common feature of neoselenodont artiodactyls, equine perissodactyls, and scandentians is the high orbit frontation values they display. As mentioned previously, vertically reorienting the orbit relative to the braincase has been argued to lead to postorbital bar formation in some carnivorans (e.g., Ravosa et al., 2000a). This type of reorientation of the orbit may also lead to a deviation away from the plane of the temporal fossa in a manner similar to that hypothesized for convergence. The examples from neoselenodont and equid evolution suggest that shifts in orbit orientation other than simply higher orbit convergence may also require the presence of an osseous structure to prevent the adjacent temporalis musculature from deforming the lateral orbital margin, thereby disrupting the normal position of the eye.

Focus of This Study

This study evaluates the hypothesis that the degrees of postorbital ossification are correlated with the angular deviation between the orbit and temporal fossa. This hypothesis has several predictions: 1) a decrease in the *orbitotemporal angle* (the angle between the orbital plane and the plane of the temporal fossa) is correlated with replacement of the postorbital ligament by bone; 2) variance in orbitotemporal angle is explained by orbit orientation; and 3) changes in relative orbit size (i.e., orbit diameter) reorient the orbit. Relative brain size, which is interpreted here to covary with braincase size, may also reorient the orbit and lead to the evolution of processes and bars (e.g., Noble et al., 2000; Ravosa et al., 2000a).

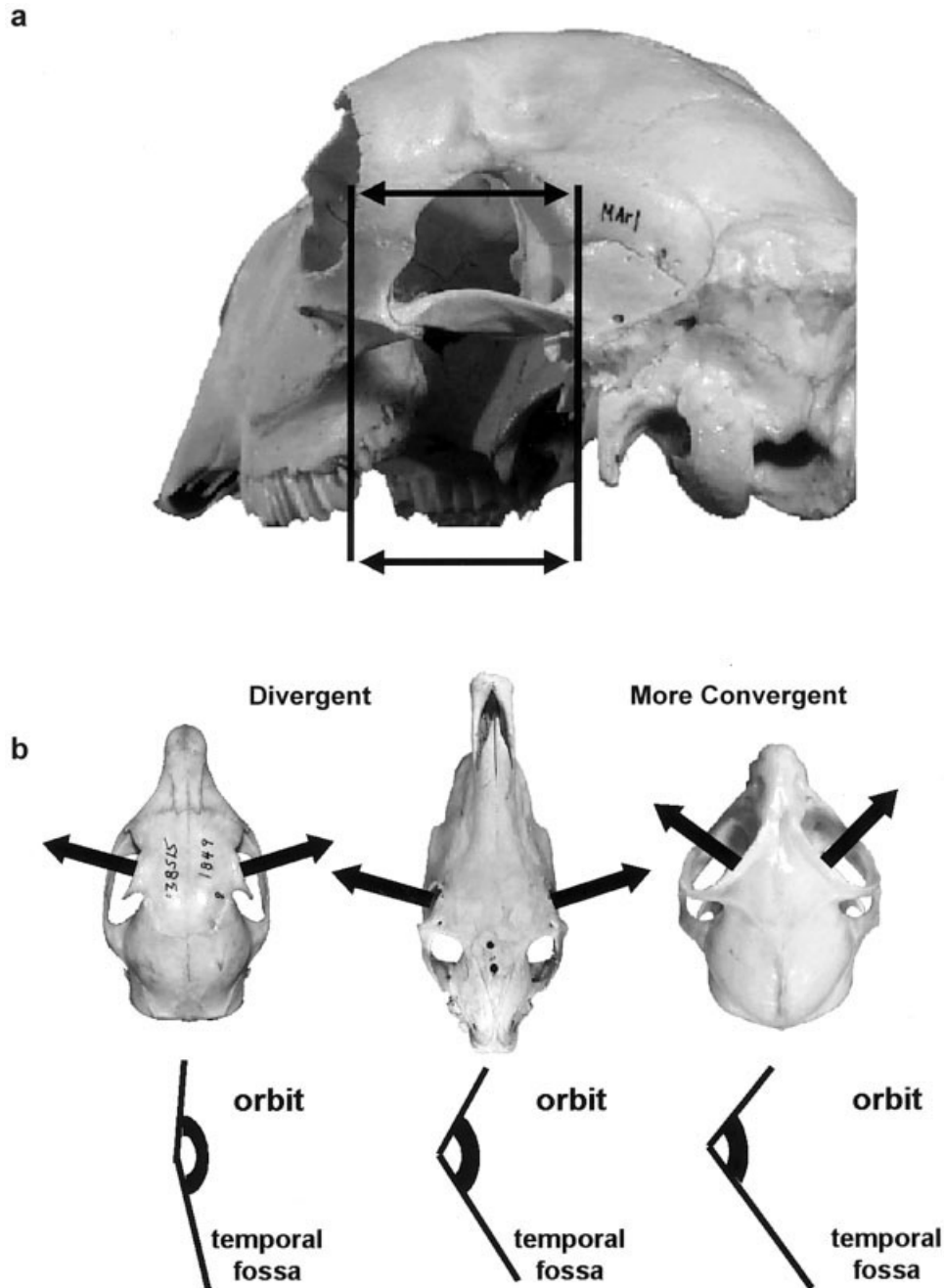


Fig. 3. Orientation of the orbit and temporal fossa in some mammals. **a:** It is hypothesized here that lateral displacement of the posterolateral orbital margin in neoselenodonts, such as *Ovis*, is similar to the deviation of the orbital and temporal fossa planes that Cartmill suggested would lead to distortions of the orbital margin in taxa with convergent orbits. This displacement is indicated by the arrowed space between the brackets. **b:** *Equus* (center) has divergent orbits, similar to *Sciurus* (left), but the orientation of the orbit relative to the temporal fossa is more similar to taxa with convergent orbits (e.g., *Otolemur*, right). Each arrow indicates the orientation of the orbital axis, which is perpendicular to the orbital plane. The angles below each skull are provided to roughly illustrate the angular relationship between the orbit and temporal plane. (Skull sizes not to scale.)

These predictions are evaluated in a representative sample of mammals using angular and linear morphometric data that characterize the size, position, and orientation of the orbit and temporal fossa to each other, as well as relative to other components of the skull.

MATERIALS AND METHODS

Taxa Sampled

Data were collected on 1,329 specimens of 321 taxa from 16 orders of extant eutherian and metatherian mammals. These orders include (number of taxa in parentheses): Artiodactyla (23), Carnivora (76), Chiroptera (32; megachiropterans only), Cingu-

lota (3), Dermoptera (2), Erinaceomorpha (5), Hyracoidea (4), Macroscelidea (7), Metatheria (29), Perissodactyla (6), Pilota (4), Primates (93; 35 strepsirrhines, 58 haplorhines), Rodentia (26), and Scandentia (11). The perissodactyls and artiodactyls both include taxa that have complete bars, such as neoselenodont artiodactyls and equid perissodactyls, and those that have postorbital processes, such as suiform artiodactyls and tapirid perissodactyls. Individual species are listed with the raw data that are available as Supplementary Material at <http://www.interscience.wiley.com/jpages/0362-2525/suppmat>. The taxa included in this study span orbit morphology from completely confluent orbitotemporal fossae, to post-orbital processes and bars. While conducting this study, four megachiropteran, one hyracoid, and eight carnivoran taxa polymorphic for processes and complete bars were measured. In the individuals of these polymorphic taxa without complete bars, the sizes of the postorbital gaps are small, usually not more than a few millimeters. These polymorphic taxa were treated individually for the simultaneous analyses of the entire data. The samples are housed in the Departments of Mammalogy of the American Museum of Natural History, Smithsonian Institution, and the Museum of Comparative Zoology (Harvard).

Measurements of Orbit Orientation and Postorbital Morphology

Two measurements of orbit orientation have been used in the primatological morphometric literature (e.g., Ross, 1995a; Ravosa et al., 2000a), both of which were first devised by Cartmill (1970). *Convergence* is defined as the dihedral angle (an angle between two planes) between the orbital margin plane (plane containing orbitale superius, orbitale anterius, and orbitale inferius) and the midsagittal plane (Fig. 4). *Frontation* is defined as the angle between the nasion-inion chord and the orbital plane as it crosses the sagittal plane (Fig. 4). For this study, an additional measure was devised called *verticality*. This measurement is defined as the dihedral angle between the orbital margin plane and palatal plane (plane containing prosthion and points taken on alveolar margin directly above the middle of each M¹). The purpose of this was to derive another dihedral angle for vertical orientation of the orbit which would be comparable to convergence but was not sensitive to displacement of inion or nasion (as frontation may be). Differences between frontation and verticality, both measures of the vertical orientation of the orbit, derive from angle definition. Frontation is a measure of orbit orientation relative to the nasion-inion chord, a line that runs roughly along the long axis of the braincase. Verticality is measured relative to the palate. Differences between verticality and frontation are probably based on differences in orientation between the face and braincase, the angle between which can differ among mammals (Cartmill, 1970, 1974; Ross and Ravosa, 1993; Ross et al., 2004).

The dihedral angle between the orbital and temporal planes (Table 1) is defined here as the *orbitotemporal angle* (Fig. 4). This is the dihedral angle between the orbital plane and an idealized temporal plane (plane containing orbitale superius, orbitale lateralis, and the posteriormost point on the temporal fossa [generally identified by the rugosity of the temporal line in the region of inion]). This measurement was derived for this study specifically to characterize the angular relationship between the orbit and temporal fossa that Cartmill described. Taxa in which the orbital and temporal planes are coplanar will have orbitotemporal angle values of 180°, whereas taxa with orbits and temporal fossae at right angles will have orbitotemporal angles of 90°.

In addition, in taxa without complete postorbital bars I measured the minimum linear distance from the tips of the ventral and dorsal postorbital processes using digital calipers to the nearest 0.1 mm. A ratio was computed with the size of the postorbital gap (a surrogate for the length of the postorbital ligament) in the numerator and the superoinferior diameter of the orbit in the denominator. This ratio is subtracted from 1. The result is a variable called the *gap-diameter ratio*. Taxa with postorbital gaps similar to orbit diameter in size, meaning small processes and large postorbital ligaments, will have very low values because the

ratio is subtracted from 1. Taxa with complete bars (and no postorbital gap) will have a value of 1. It should be noted that ratio data can potentially conform to a non-normal distribution, requiring the arcsin transformation to approximate a normal distribution (Sokal and Rohlf, 1995). A comparison between the raw ratio and arcsin transformed ratio data demonstrated that these were identical. This being the case, the raw ratio data were used for all analyses.

Coordinate Data Preparation

Three-dimensional coordinate data were collected for 22 landmark points on the skull with a MicroScribe-3DX coordinate data stylus (Immersion, San Jose, CA). Each specimen was mounted on an elevated clay base so that all coordinate data could be collected in a single series (Lockwood et al., 2002). Each specimen sits within its own 3D coordinate data space with this arrangement. These coordinate points were transformed into linear, angular, and volume measurements (Table 1; raw data are available as Supplementary Material at <http://www.interscience.wiley.com/jpages/0362-2525/suppmat>). Linear data were calculated from coordinates using the distance formula. Estimates of braincase volume were derived from linear measurements using an ellipsoidal shell model.

Taxa included in this study spanned a substantial range of sizes. In order to compare shape changes of the skull in relation to orbit orientation, size adjustment of linear data was conducted by dividing each linear variable of a specimen by the geometric mean of all 14 linear measurements for that specimen (Corrucini, 1995; Jungers et al., 1995; Table 1). The result is a dimensionless geometric expression of shape and relative size (Corrucini, 1995). Additionally, angular data can potentially be non-normally distributed due to the constraints of circular dimensions (Fisher, 1993). Departures from normality for angular and linear data were tested using the Kolmogorov-Smirnov test with Lilliefors modification (Sokal and Rohlf, 1995). In several orders angular measures deviated moderately from normality, but not to a degree that required a specialized statistical distribution (e.g., Fisher, 1993). Nonparametric alternatives were used instead.

Data Analysis

In order to investigate the relationships between variables, Spearman's rank correlation coefficients were calculated. Variables in this study were found to show patterns of intercorrelation. Correlations between variables can be due to the effects of other independent variables (Sokal and Rohlf, 1995; Hair et al., 1998). These were evaluated using partial correlation coefficients.

Both nonphylogenetic and phylogenetic approaches were used for bivariate correlation analyses. Continuous biological data potentially violate standard statistical assumptions of independence due to phylogenetic relatedness (Felsenstein, 1985). Data were adjusted for phylogenetic similarity with the method of phylogenetic generalized least squares (PGLS, Martins and Hansen, 1997; Rohlf, 2001) using COMPARE 4.4 (Martins, 2001). The PGLS method is based on normal least-squares regression but with a specialized error term that is a function of the variance matrix and phylogenetic relationships of all included taxa. Rohlf (2001) demonstrated that the more commonly used method of phylogenetic independent contrasts (Felsenstein, 1985) is a special case of PGLS, but that the generalized least-squares method is not limited to the assumption of the Brownian motion continuous random walk model of evolution.

Phylogenetic data on megachiropterans are from Jones et al. (2002). Carnivoran phylogenetic data are from Bininda-Emonds et al. (1999), with adjustments to viverrid and herpestid taxa to maintain Malagasy carnivoran monophyly based on Yoder et al. (2003). Primate data are from Purvis (1995; Purvis and Webster, 1999). Sciurid phylogenetic data (excluding the Anomaluridae) are from Mercer and Roth (2003) based on their Bayesian derived tree. Metatherian phylogenetic data are a composite taken from multiple sources (Kirsch et al., 1993; Springer et al., 1994; Patton

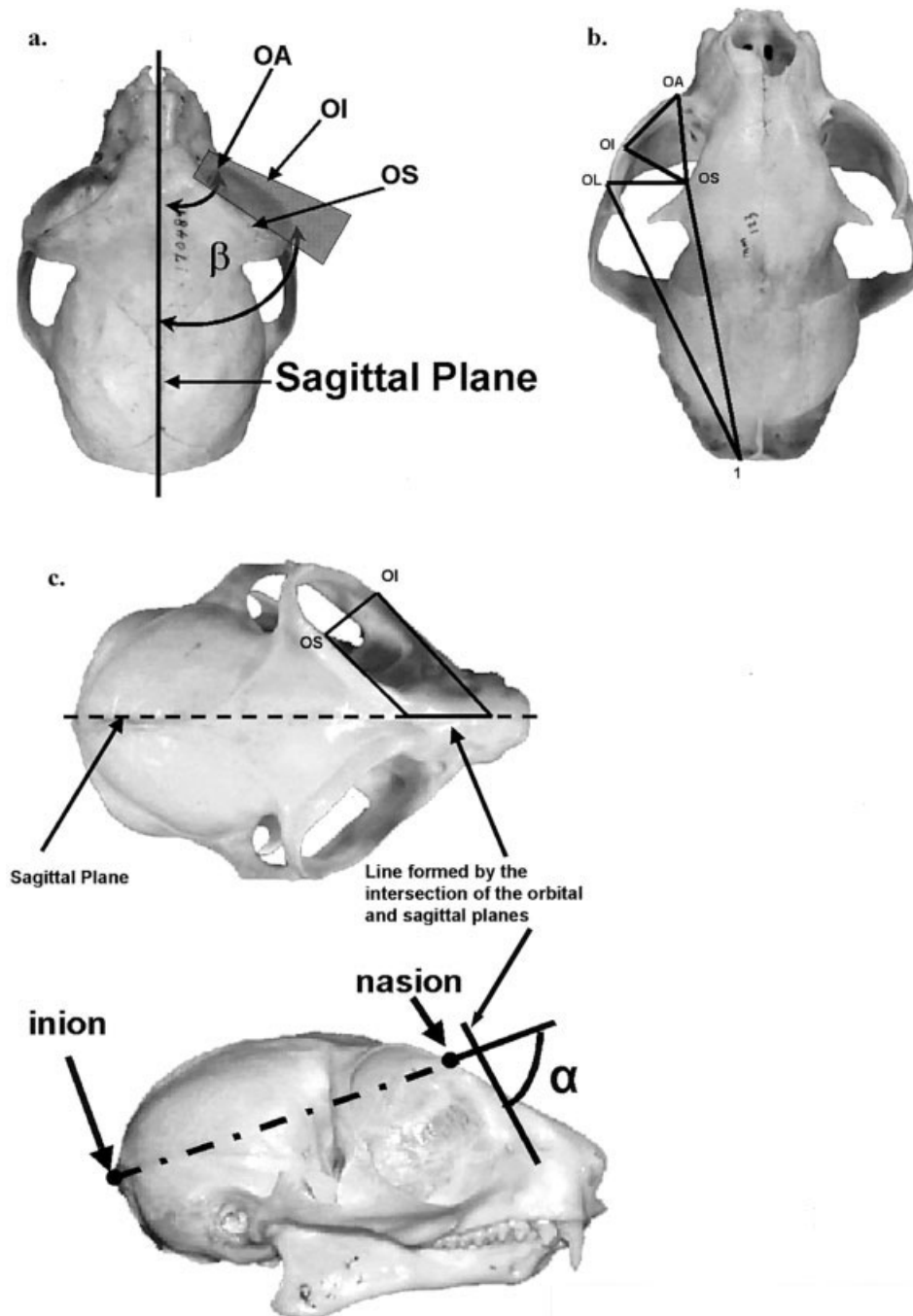


Fig. 4. Angular measurements. **a:** Convergence is the dihedral angle between the orbital and sagittal planes. Note that verticality (not shown) is similar in that it is the dihedral angle between the orbital and palatal planes (plane containing prosthion and points taken along the alveolar margin directly above the middle of each M^1). **b:** Orbitotemporal angle is the dihedral angle between the orbital and temporal fossa planes. **c:** Frontation is the angle between the nasion-inion chord and the line formed by the intersection of the orbital and sagittal planes. OS, orbitale superius, point on the orbital margin furthest from the tooththrow; OI, orbitale inferius, point on the bony orbital margin closest to the tooththrow; OA, orbitale inferius, point on the bony margin most distant from inion; OL, orbitale lateralis, lateralmost point on the bony margin; α , frontation angle; β , convergence angle. (Skulls not to scale.)

et al., 1996; McKenna and Bell, 1997; Hamilton and Springer, 1999). Cetartiodactyl phylogenetic data are a composite taken from multiple sources (Randi et al., 1996; Hassanin and Douzery, 1999, 2003). Trees that were assembled for this study or substantially modified to contain only those taxa included in this project are available as Supplementary Material at

www.interscience.wiley.com/jpages/0362-2525/suppmat. The PGLS analyses for metatherians exclude *Chironectes*, which was not present in the molecular trees. In several cases among metatherians, taxa not included in the molecular tree were manually inserted under the assumption of generic monophyly. Polychotomous relationships were arbitrarily resolved and rel-

TABLE 1. Measurements and derived variables used in this study

Measurements and variables	Definitions
Skull length (si)	Distance from prosthion to inion
Nasion-Inion (ni)	Distance from nasion to inion
Prosthion-Nasion (pn)	Distance from prosthion to nasion
Interorbital width (iw)	Distance between the most medial points on each orbital margin
Orbit diameter (od)	Distance from orbitale superius to orbitale inferius
Orbit depth (odp)	Distance from midpoint of orbit diameter to optic foramen
Bioptic foramen width (bf)	Distance from superior margin of each optic foramen
Temporal fossa length (tl)	Distance from the anterior temporal line midcurve along the dorsal postorbital process to the posteriormost point on the temporal fossa [generally identified by the rugosity of the temporal line in the region of inion]).
Temporal fossa width (tw)	$tw = (\text{bizygomatic distance} - po) / 2$
Bizygomatic width (bw)	Maximum width across the zygomatic arches
Postorbital width (po)	Minimum distance between points posterior to the postorbital processes or bars, or slope between anterior aspect of braincase before entering the orbit.
Bitemporal distance (bt)	Maximum coronally oriented bitemporal distance
Biporionic distance (bp)	Distance between the left and right porion (Ext. Acoustic Meatus)
Braincase length (bl)	Distance from midpoint of line <i>po</i> (postorbital width) to inion
Skull geometric mean	$(si * ni * pn * iw * od * odp * bf * tl * tw * bw * po * bt * bp * bl)^{1/14}$
Postorbital gap	Distance between the tips of the ventral and dorsal postorbital processes (a surrogate for the length of the postorbital ligament).
Cube root of braincase volume	Cube root of the estimated braincase volume from external dimensions. Braincase volume was modeled as an ellipsoid, $V = 4/3abc$. <i>a</i> is 1/2 the length of the line from the midpoint between points of postorbital constriction to inion. <i>b</i> is 1/2 the biporionic distance. <i>c</i> is the from bregma to midpoint of biporionic line.
Convergence of orbits	Dihedral angle between the orbital margin plane (plane containing orbitale anterius, orbitale superius and orbitale inferius) and the midsagittal plane (plane containing prosthion, nasion, and inion).
Frontation of orbits	Angle between the nasion-inion chord and the orbital plane as it crosses the sagittal plane.
Verticality of orbits	Dihedral angle between the orbital margin plane and palatal plane (plane containing prosthion, and points taken along the alveolar margin directly above the middle of each M^1).
Orbitotemporal angle	Dihedral angle between the orbital plane and the temporal plane (plane containing orbitale superius, orbitale lateralis, and the posteriormost point on the temporal fossa [generally identified by the rugosity of the temporal line in the region of inion]).

Definitions of anatomical landmarks follow Hershkovitz (1977). Definitions of convergence and frontation are from Cartmill (1970). Orbitale anterius is the point on the orbital margin most distant from inion. Orbitale superius is the point on the orbital margin farthest from the alveolar margin, and orbitale inferius is the point on the orbital margin closest to the alveolar margin.

atively very small branch lengths supplied following Martins (2001). Both nonphylogenetic and phylogenetically adjusted data are presented, and in those cases where adjustment implies another statistical relationship, the relationships are discussed.

Compatibility and Replicability of Orbit Orientation Measurements

Previous studies of orbit orientation in mammals (Cartmill, 1970; Ross, 1995a; Noble et al., 2000; Ravosa et al., 2000b) measured orbit orientation using a dihedral goniometer designed and built by Drs. Matt Cartmill and Charles Oxnard for Cartmill's dissertation research. This instrument is unique, and it is reasonable to question whether the dihedral measurements made from it are equivalent to those computed from the 3D coordinates collected using the MicroScribe 3DX coordinate data stylus. In

order to evaluate this, convergence and frontation angles collected by Dr. Callum Ross using the dihedral goniometer were compared with data collected during this project. This comparison was restricted to 41 identical primate taxa. Ross's and this projects' convergence and frontation measurements are highly correlated ([Convergence, Spearman's rho = -0.966, $P \ll 0.001$, $n = 41$], [Frontation, Spearman's rho = -0.966, $P \ll 0.001$, $n = 41$]). In addition, the slopes are indistinguishable from 1. These data suggest that measurements made using each instrument are equivalent.

The replicability of measuring the angles of orbit convergence (a dihedral angle) and orbit frontation (an angle between a line and a plane) was evaluated by taking each measurement six times on six skulls of *Alouatta seniculus*. Overall analyses of variance (ANOVA) for each variable were significant (Convergence: $F(5,30) = 32.65$, $P \ll 0.01$; Frontation: $F(5,30) = 122.06$, $P \ll 0.01$), indicating that there are significant differences between mean variable values among specimens. Because each

TABLE 2. Correlation statistics: nonphylogenetic and PGLS results

Taxon	<i>n</i>		Convergence	Frontation	Verticality	Orbit diameter ^a	Orbitotemporal angle	Gap-diameter ratio	³ Braincase volume ^a	Braincase length ^a	Postorbital constriction ^a	Temporal fossa width ^a		
All Taxa	324	Convergence	—	0.519**	0.119*	-0.082	-0.718**	0.358**	0.453**	0.551**	0.186**	0.041		
		Frontation		—	0.681**	-0.019	-0.916**	0.724**	0.452**	0.369**	0.420**	-0.260**		
		Verticality			—	-0.194**	-0.542**	0.609**	0.428**	0.186**	0.646**	-0.518**		
		Orbit diameter				—	-0.042	0.166**	0.211**	-0.125*	0.212**	-0.123*		
		OT angle					—	-0.752**	-0.491**	-0.375**	-0.455**	0.275**		
		Gap-diam ratio						—	0.502**	0.185**	0.634**	-0.502**		
		³ Braincase volume							—	0.624**	0.580**	-0.101		
		Braincase length								—	-0.046	0.354**		
		Constriction									—	-0.821**		
		TFWidth										—		
		Metatheria	29	Convergence	—	0.172	-0.589**	0.047	-0.304	0.124	0.256	0.369*	-0.569**	0.455*
		28	Frontation	0.047	—	0.433*	-0.114	-0.938**	0.347	0.082	0.204	-0.074	0.128	
			Verticality	-0.508**	0.716**	—	-0.113	-0.312	0.170	-0.276	-0.230	0.439*	-0.368*	
Orbit diameter	-0.312		-0.207	-0.022	—	0.062	0.477**	0.456*	0.230	-0.006	0.484**			
OT angle	-0.213		-0.964**	-0.547**	0.225	—	-0.297	-0.144	-0.159	0.103	-0.201			
Gap-diam ratio	0.100		0.377*	0.257	0.250	-0.396*	—	-0.085	-0.055	0.140	0.049			
³ Braincase volume	-0.065		-0.258	-0.200	0.413*	0.299	-0.377*	—	0.797**	-0.404*	0.818**			
Braincase length	0.245		0.043	-0.206	0.077	0.095	-0.122	0.712**	—	-0.613**	0.727**			
Constriction	-0.285		0.294	-0.530**	-0.114	-0.274	0.299	-0.654**	-0.721**	—	-0.740**			
TFWidth	0.079		-0.361*	-0.421*	0.339	0.334	-0.390*	0.905**	0.637**	-0.879**	—			
Chiroptera	36		Convergence	—	-0.014	-0.425**	-0.360*	-0.688**	0.373*	0.290	0.594**	-0.538**	0.613**	
21	Frontation		0.037	—	0.614**	-0.324	-0.539**	0.405**	0.167	-0.060	0.017	0.129		
	Verticality		-0.378*	0.704**	—	0.614**	-0.013	-0.187	0.055	-0.296	0.397*	-0.272		
	Orbit diameter		-0.263*	-0.407*	0.042	—	0.414*	-0.428**	-0.289	-0.581**	0.443**	-0.478**		
	OT angle	-0.772**	-0.680**	-0.195	0.461**	—	-0.652**	-0.332*	-0.474**	0.497**	-0.637**			
	Gap-diam ratio	0.462**	0.366*	-0.173	-0.398*	-0.567**	—	0.159	0.418*	-0.627**	0.634**			
	³ Braincase volume	0.232	0.206	0.067	-0.323	-0.234	-0.230	—	0.454**	-0.064	0.488**			
	Braincase length	0.550**	0.235	-0.110	-0.506**	-0.405*	0.049	0.716**	—	-0.778**	0.823**			
	Constriction	-0.586**	-0.051	0.318	0.309	0.304	-0.565**	-0.093	-0.671**	—	-0.855**			
	TFWidth	0.664**	0.154	-0.263	-0.406*	-0.675**	0.605**	0.568**	0.625**	-0.850**	—			
	Carnivora	84	Convergence	—	0.209	-0.492**	0.470**	-0.686**	0.084	-0.273*	-0.418**	0.291**	-0.482**	
	74	Frontation	0.304**	—	0.589**	0.181	-0.766**	0.740**	0.163	-0.083	0.550**	-0.333**		
		Verticality	-0.211	0.625**	—	-0.299**	-0.130	0.512**	0.344**	0.230*	0.236*	0.086		
		Orbit diameter	0.090	0.226	0.061	—	-0.405**	0.297**	0.101	-0.062	0.405**	-0.296**		
OT angle		-0.662**	-0.362**	-0.327**	—	-0.573**	0.122	0.445**	-0.615**	0.599**	—			
Gap-diam ratio		0.213	0.554**	0.441**	0.392**	-0.505**	—	0.132	-0.058	0.446**	-0.343**			
³ Braincase volume		-0.010	0.278*	0.209	0.240*	-0.118	0.179	—	0.676**	0.173	0.584**			
Braincase length		-0.136	-0.041	0.081	0.020	0.205	0.016	0.718**	—	-0.370**	0.705**			
Constriction		0.141	0.516**	0.343**	0.355**	-0.550**	0.389**	0.226	-0.337**	—	-0.587**			
TFWidth		-0.111	-0.229	-0.187	-0.128	0.386**	-0.225	0.590**	0.709**	-0.660**	—			
Artiodactyla		23	Convergence	—	-0.542**	-0.660**	-0.369	0.315	-0.387	-0.259	-0.193	-0.252	0.256	
21		Frontation	-0.588**	—	0.930**	0.355	-0.872**	0.676**	0.383	0.194	0.428*	-0.056		
		Verticality	-0.689**	0.914**	—	0.350	-0.770**	0.618**	0.382	0.188	0.393	-0.118		
		Orbit diameter	-0.275	-0.016	0.086	—	-0.425*	0.678**	0.806**	0.600**	0.831**	-0.529**		
	OT angle	0.199	-0.718**	-0.624**	0.009	—	-0.685**	-0.422*	-0.166	-0.567**	0.261			
	Gap-diam ratio	-0.298	0.320	0.407	0.406	-0.275	—	0.747**	0.493*	0.740**	-0.212			
	³ Braincase volume	-0.185	0.080	0.062	0.796**	0.085	0.363	—	0.837**	0.879**	-0.399			
	Braincase length	-0.057	-0.098	-0.124	0.286	0.478*	0.083	0.692**	—	0.578**	-0.172			
	Constriction	-0.264	0.152	0.153	0.906**	-0.276	0.389	0.895**	0.497*	—	-0.615**			
	TFWidth	0.268	-0.051	-0.101	-0.680**	0.391	-0.196	-0.448**	-0.247	-0.765**	—			
	Rodentia	26	Convergence	—	0.339	-0.382	0.188	-0.459*	0.186	0.099	0.460*	-0.556**	0.634**	
	21	Frontation	0.144	—	0.273	-0.192	-0.843**	0.691**	0.177	0.769**	-0.649**	0.694**		
		Verticality	-0.581**	-0.057	—	-0.273	-0.168	0.465*	0.092	0.062	0.278	-0.271		
		Orbit diameter	0.170	0.220	-0.269	—	0.102	-0.216	0.382	-0.003	0.169	-0.011		
OT angle		-0.390	-0.862**	-0.269	0.172	—	-0.672**	-0.183	-0.751**	0.761**	-0.862**			
Gap-diam ratio		-0.026	0.756**	0.292	0.038	-0.803**	—	0.214	0.653**	-0.446*	0.459*			
³ Braincase volume		0.203	0.166	-0.155	0.497*	0.091	0.143	—	0.290	0.218	0.115			
Braincase length		0.442*	0.764**	-0.127	-0.148	-0.519*	0.540**	0.125	—	-0.708**	0.713**			
Constriction		-0.506*	-0.691**	0.235	0.254	0.686**	-0.180	0.244	-0.824**	—	-0.908**			
TFWidth		0.628**	0.165	-0.211	0.285	-0.075	0.131	-0.214	-0.824**	-0.608**	—			
Scandentia		11	Convergence	—	0.427	-0.255	-0.582	-0.636*	-0.718**	0.055	-0.736**	0.718*		
11		Frontation		—	0.664*	-0.564	-0.891**	-0.891**	-0.055	0.682*	-0.355	0.445		
		Verticality			—	-0.236	-0.427	-0.427	0.400	0.727*	0.091	-0.018		
		Orbit diameter				—	0.691*	—	0.755**	-0.591	0.864**	-0.900**		
	OT angle					—	—	0.373	-0.645*	0.573	-0.609*			
	Gap-diam ratio						—	—	-0.100	0.918**	-0.873**			
	³ Braincase volume							—	—	-0.373	0.418			
	Braincase length								—	—	-0.982**			
	Constriction									—	—			
	TFWidth										—			

(continued)

overall *F*-test was significant, follow-up tests were conducted to evaluate pairwise differences among the means. Results from both Tukey's-b (equal variances assumed) and Dunnett's C (does not assume equal variances) demonstrate that individuals could be distinguished by the means of the variables. These results support the replicability of the measurement technique because individuals could be distinguished by the means of multiple measurements.

RESULTS

Variation in Orbitotemporal Orientation

Orbitotemporal angle is compared to convergence, frontation, and verticality in order to evaluate how changes in orbit orientation affect the angle between

TABLE 2. (Continued)

Taxon	<i>n</i>	Convergence	Frontation	Verticality	Orbit diameter ^a	Orbitotemporal angle	Gap-diameter ratio	³ Braincase volume ^a	Braincase length ^a	Postorbital constriction ^a	Temporal fossa width ^a	
Primates Strepsirrhini	35	Convergence	—	0.138	-0.080	-0.428*	-0.387*	-0.264	0.296	-0.575**	0.261	
		Frontation	<i>0.102</i>	—	0.650**	-0.379*	-0.848**	-0.373*	-0.306	0.014	-0.311	
		Verticality	<i>-0.089</i>	<i>0.654**</i>	—	-0.055	-0.510**	-0.034	-0.158	0.216	-0.294	
		Orbit diameter	<i>-0.497**</i>	<i>-0.113</i>	<i>0.177</i>	—	0.512**	0.754**	0.019	0.415*	0.332	
		OT angle	<i>-0.454**</i>	<i>-0.805**</i>	<i>-0.426**</i>	<i>0.179</i>	—	0.511**	0.140	0.186	0.303	
		Gap-diam ratio	—	—	—	—	—	—	—	—	—	—
		³ Braincase volume	<i>-0.274</i>	<i>-0.147</i>	<i>0.190</i>	<i>0.669**</i>	<i>0.262</i>	—	—	0.322	0.441**	0.338*
		Braincase length	<i>0.246</i>	<i>-0.270</i>	<i>-0.112</i>	<i>-0.086</i>	<i>0.218</i>	0.280	—	-0.347*	0.390*	
		Constriction	<i>-0.553**</i>	<i>0.021</i>	<i>0.159</i>	<i>0.499**</i>	<i>0.178</i>	<i>0.618**</i>	<i>-0.308</i>	—	-0.572**	
		TFWidth	<i>0.358*</i>	<i>-0.084</i>	<i>0.031</i>	<i>0.115</i>	<i>-0.091</i>	<i>0.336*</i>	<i>0.346*</i>	<i>-0.620**</i>	—	
		Primates Haplorhini	58	Convergence	—	0.177	0.169	-0.540**	-0.635**	-0.564**	-0.235	-0.670**
Frontation	<i>0.103</i>			—	0.711**	-0.414**	-0.783**	-0.141	0.190	-0.160	0.085	
Verticality	<i>0.264*</i>			<i>0.708**</i>	—	-0.399**	-0.578**	-0.242	0.022	-0.161	0.069	
Orbit diameter	<i>-0.493**</i>			<i>-0.298*</i>	<i>-0.549**</i>	—	0.568**	0.661**	0.208	0.809**	-0.648**	
OT angle	<i>-0.673**</i>			<i>-0.746**</i>	<i>-0.587**</i>	<i>0.281*</i>	—	0.392**	0.001	0.452**	-0.334*	
Gap-diam ratio	—			—	—	—	—	—	—	—	—	—
³ Braincase volume	<i>-0.460**</i>			<i>-0.208</i>	<i>-0.357**</i>	<i>0.410**</i>	<i>0.520**</i>	—	0.684**	0.826**	-0.451**	
Braincase length	<i>-0.088</i>			<i>-0.026</i>	<i>-0.182</i>	<i>-0.054</i>	<i>0.200</i>	0.679**	—	0.385**	-0.178	
Constriction	<i>-0.641**</i>			<i>-0.208</i>	<i>-0.421**</i>	<i>0.759**</i>	<i>0.480**</i>	<i>0.762**</i>	<i>0.271</i>	—	-0.813**	
TFWidth	<i>0.513**</i>			<i>0.047</i>	<i>0.276*</i>	<i>-0.598**</i>	<i>-0.182</i>	<i>-0.196</i>	<i>0.015</i>	<i>-0.770**</i>	—	

Spearman's rho * $P < 0.05$; ** $P < 0.01$.

^aLinear variables are ratios as these have been divided by the geometric mean of all linear data.

Italicized correlation coefficients (bottom left) are phylogenetic generalized least-squares values and normal faced (top right) are nonphylogenetic Spearman's rank correlation coefficients. Note that the sample size for the 'All Taxa' block of analyses includes polymorphic species. Only variables that displayed significant correlations are included.

the orbit and the temporal fossa. In addition, orbitotemporal angle is compared to other linear variables that may influence the angular relationship between the orbit and temporal fossa. Emphasis is placed on patterns of correlations that are generally supported across mammals as well as identifying the notable deviations from these general patterns.

Orbitotemporal angle is significantly negatively correlated with orbit convergence (Table 2: All Taxa; Fig. 5). These data indicate that, across eutherian mammals, the more the orbits face in the same direction, the more the orbital plane deviates from the plane of the temporal fossa. Neoselenodont artiodactyls and equid perissodactyls appear to deviate from the general mammalian trend. Among these ungulate taxa there is a nonsignificant correlation between these variables (see, for example, Table 2: Artiodactyla). These taxa have lower orbitotemporal angles than is expected for their values of convergence (which are generally low). It is worth noting that these are the two groups of artiodactyls and perissodactyls that have evolved complete postorbital bars.

Orbitotemporal angle is significantly negatively correlated with frontation (Table 2: All Taxa; Fig. 6). These data indicate that the closer to vertical the orbital plane is relative to the braincase, the more the orbit deviates from the temporal fossa. A similar relationship between orbitotemporal angle and orbit verticality is found (Table 2: All Taxa; Fig. 7). However, there is less variance in orbitotemporal angle explained by verticality than by frontation. These data on orbitotemporal angle and verticality indicate that higher vertical orientation of the orbit relative to the palate also leads to greater deviation between the orbital and temporal planes. The exceptions to this are artiodactyls and primates, neither of which has a significant

relationship between orbitotemporal angle and verticality. Among metatherians, a negative correlation between frontation and orbitotemporal angle is the only significant relationship directly affecting the deviation of the orbit from the temporal fossa. This implies that in metatherians, a group that generally has high orbit convergence (Heesy, 2003), the predominant change in orbit orientation that leads to low orbitotemporal angle is the rotation of the orbital plane relative to the long axis of the braincase.

When correlations between orbitotemporal angle and linear variables across mammals are compared to those found for individual groups, a complex series of relationships is suggested. For example, relative orbit diameter and orbitotemporal angle are negatively correlated in carnivorans and artiodactyls, whereas these are positively correlated in other groups such as chiropterans, scandentians, and primates. In taxa with a negative correlation between these variables, increases in relative orbit diameter lead to greater angular deviation between the planes of the orbit and temporal fossa. The opposite is indicated in taxa with a positive correlation between relative orbit diameter and orbitotemporal angle. Similarly, at least one measure of relative braincase size (volume or length) is correlated with orbitotemporal angle among eutherian taxa (Table 2). In chiropterans and artiodactyls, relative braincase volume is negatively correlated with orbitotemporal angle, which is interpreted as the orbit and temporal fossa deviating more with increasing braincase volume. Primates and carnivorans show the opposite pattern: increasing relative braincase size leads to a larger orbitotemporal angle, or less deviation between the orbit and temporal fossa.

It is particularly interesting to note that there is no general allometric relationship between orbitotemporal angle and the geometric mean of skull size (a surrogate of overall skull size) across metatherian and eutherian mammals. Although the correlation between orbitotemporal angle and the geometric mean of skull size is significant (Spearman's $\rho = -0.203$, $P < 0.01$, $n = 334$), this is driven by the substantial sample size. Only among anthropoid and strepsirrhine primates is there a relationship between orbitotemporal angle and the geometric mean of skull size (Spearman's $\rho = -0.483$, $P < 0.01$, $n = 93$). This latter result is probably derived from the significant correlation between orbit size and the geometric mean of skull size in primates (Spearman's $\rho = -0.907$, $P \leq 0.01$, $n = 93$). Nevertheless, these results demonstrate that variation in orbitotemporal angle is not related to size. It could additionally be argued that size-based reorientation of the orbitotemporal angle could be associated with the size and orientation of the temporal fossa. Dietary ecology could therefore affect orbitotemporal angle. However, $\sim 92\%$ of the variance in orbitotemporal angle is explained by orbit convergence, frontation, and verticality, when analyzed simultaneously using multiple regression ([orbitotemporal angle] = $195.05 - 0.424$ [convergence] - 0.614 [frontation] - 0.116 [verticality]; $F(3,330) = 1243.719$, $P \leq 0.001$). Most variance in orbitotemporal angle is explained by reorientation of the orbit.

Orbit Orientation and Postorbital Process Evolution

Orbitotemporal angle. Orbitotemporal angle is compared to the gap-diameter ratio in order to eval-

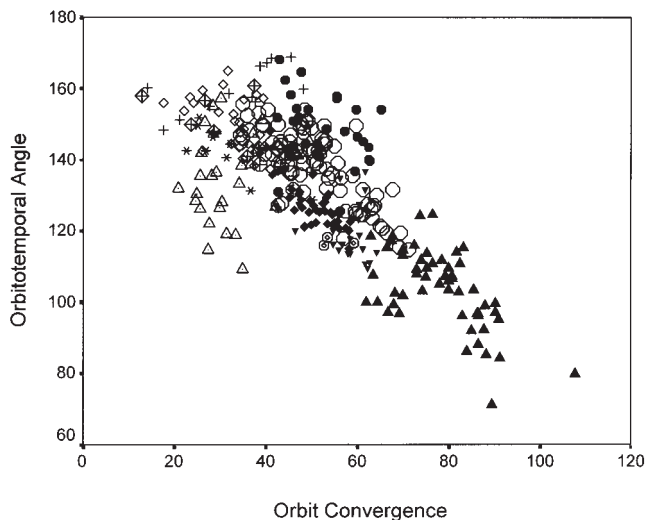


Fig. 5. Relationship between convergence and orbitotemporal angle. Both variables are plotted in degrees. \blacktriangle , Anthropeoidea; \circ , Carnivora; \blacklozenge , Chiroptera; \otimes , Dermoptera; \diamond , Epitheria; \square , Hyracoidea; $+$, Macroscelidea and Erinaceomorpha; \bullet , Metatheria; \diamond , Rodentia; $*$, Scandentia; \blacktriangledown , Strepsirrhini; \odot , Tarsiiformes; \triangle , Artiodactyla and Perissodactyla.

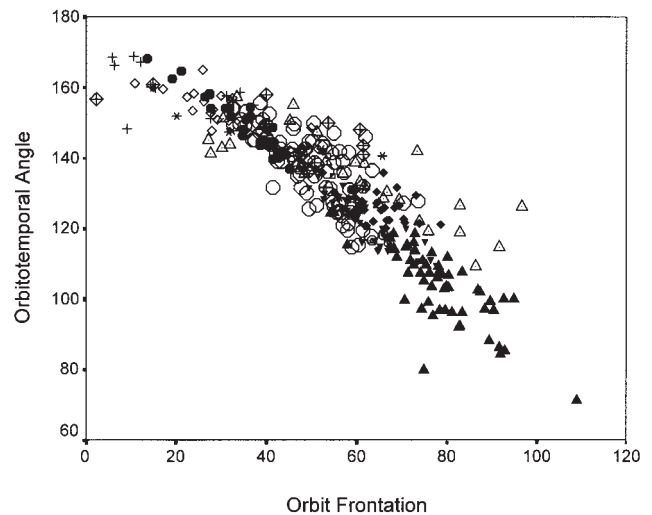


Fig. 6. Relationship between frontation and orbitotemporal angle. Both variables are plotted in degrees. \blacktriangle , Anthropeoidea; \circ , Carnivora; \blacklozenge , Chiroptera; \otimes , Dermoptera; \diamond , Epitheria; \square , Hyracoidea; $+$, Macroscelidea and Erinaceomorpha; \bullet , Metatheria; \diamond , Rodentia; $*$, Scandentia; \blacktriangledown , Strepsirrhini; \odot , Tarsiiformes; \triangle , Artiodactyla and Perissodactyla.

uate the prediction that a decrease in the angle between the orbital plane and the plane of the temporal fossa is correlated with the relative size of the postorbital processes.

Orbitotemporal angle is highly negatively correlated with the gap-diameter ratio when all taxa are analyzed together (Table 2: All Taxa; Fig. 8). This particular correlation analysis is restricted to the nonphylogenetic statistical procedure because there is not a resolved phylogeny including all of these taxa. Roughly half of the variance in postorbital gap size is explained by orbitotemporal angle (Spearman's $\rho = -0.752$, $P < 0.001$, $n = 334$). This analysis suggests that the deviation of the orbit away from the temporal plane probably leads to replacement of the postorbital ligament by postorbital processes. It is additionally noteworthy that, whereas taxa exist with orbitotemporal angles below 114° (many of which are anthropoid primates), there are no taxa without bars in this range (Fig. 8). Most taxa with postorbital processes have orbitotemporal angles in the range 120 – 170° .

As was demonstrated in the previous section, convergence, frontation, and verticality are all correlated with orbitotemporal angle. Variance in the gap-diameter ratio is not simply due to variance in these three measures. A partial correlation analysis between orbitotemporal angle and gap-diameter ratio, holding constant these measures of orbit orientation, is significant (partial correlation coefficient = -0.424 , $P < 0.001$, $n = 329$).

Megachiropterans and carnivorans are two orders with substantial variance in orbitotemporal angle and postorbital process size. These are also two of the three groups that contain taxa that are polymor-

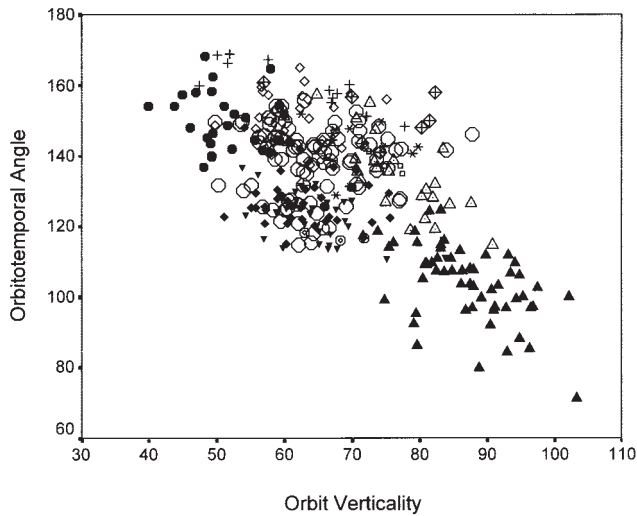


Fig. 7. Relationship between verticality and orbitotemporal angle. Both variables are plotted in degrees. \blacktriangle , Anthroipoidea; \circ , Carnivora; \blacklozenge , Chiroptera; \otimes , Dermoptera; \blacklozenge , Epitheria; \square , Hyracoidea; $+$, Macroscelidea and Erinaceomorpha; \bullet , Metatheria; \diamond , Rodentia; $*$, Scandentia; \blacktriangledown , Strepsirrhini; \odot , Tarsiiformes; \triangle , Artiodactyla and Perissodactyla.

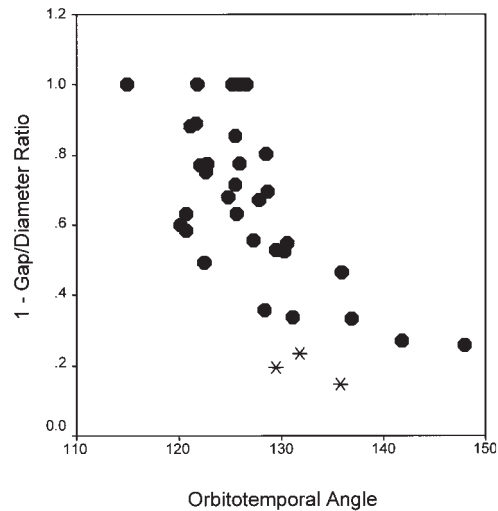


Fig. 9. Relationship between orbitotemporal angle and the ratio of postorbital gap size and orbit diameter in megachiropterans. Orbitotemporal angle is plotted in degrees. The sizes of the postorbital processes are highly negatively correlated with angle between the orbit and the temporal plane in megachiropterans (Spearman's $\rho = -0.652$, $P < 0.001$, $n = 36$). Whereas visual examination indicates that this relationship is slightly curvilinear, fitting curves to the data (such as a power relationship) does not explain significantly more variance than a linear fit. $*$, Macrogllossinae; \bullet , Pteropodinae.

phic in postorbital process-bar morphology, the other group being hyracooids. Among megachiropterans, orbitotemporal angle is highly negatively correlated with the gap-diameter ratio (Fig. 9). This indicates that, as with the interordinal analysis, the deviation of the orbit away from the temporal plane

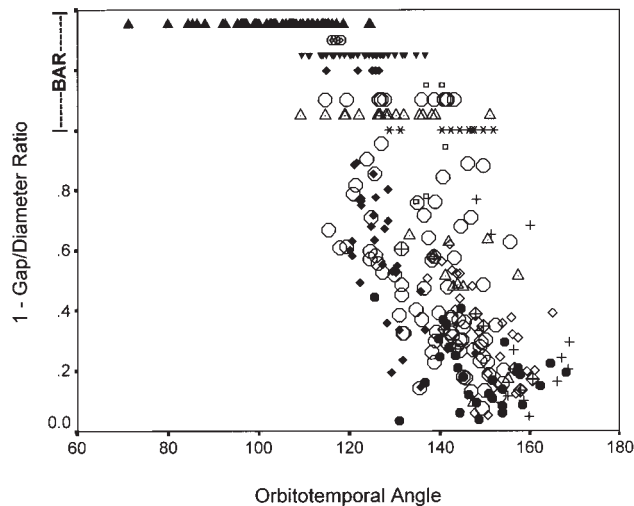


Fig. 8. Relationship between orbitotemporal angle and the ratio of postorbital gap size and orbit diameter. Orbitotemporal angle is plotted in degrees. All taxa in the 'BAR' region of the graph have a value of 1 on the y-axis. The sizes of the postorbital processes are highly negatively correlated with angle between the orbit and the temporal plane (Spearman's $\rho = -0.752$, $P < 0.001$, $n = 334$). \blacktriangle , Anthroipoidea; \circ , Carnivora; \blacklozenge , Chiroptera; \otimes , Dermoptera; \blacklozenge , Epitheria; \square , Hyracoidea; $+$, Macroscelidea and Erinaceomorpha; \bullet , Metatheria; \diamond , Rodentia; $*$, Scandentia; \blacktriangledown , Strepsirrhini; \odot , Tarsiiformes; \triangle , Artiodactyla and Perissodactyla.

leads to replacement of the postorbital ligament by postorbital processes. Whereas visual examination indicates that this relationship is slightly curvilinear, fitting curves (such as a power relationship) to the data does not explain significantly more variance than a linear fit. It is also noteworthy that although megachiropteran orbitotemporal angle values range from 115–148°, taxa with complete bars, including polymorphic individuals, inhabit the lowest part of the range from 115–125°.

The carnivoran data are similar to those of megachiropterans, with the additional result that there are two overlapping distributions present within carnivorans (Fig. 10). In the majority of carnivoran families (taken from both feliform and caniform suborders), orbitotemporal angle and the gap-diameter ratio are highly negatively correlated (Fig. 10a). This is also true of herpestid carnivorans (Fig. 10b). However, the distribution of herpestids is shifted to higher orbitotemporal angle values. The result is that herpestids that form complete postorbital bars do so at higher orbitotemporal values than is true of other carnivoran families. In both subsets of carnivorans the taxa that form bars are at the low end of the range for orbitotemporal angle.

The sample sizes for artiodactyls and perissodactyls included in this study are small. Among perissodactyls, the range in orbitotemporal angle for *Equus* species (taxa with bars) is 128–135°, whereas the most closely related taxa in this study, *Tapirus* species (which do not have bars) is 147–155°. Small sample sizes preclude the use of statistics to com-

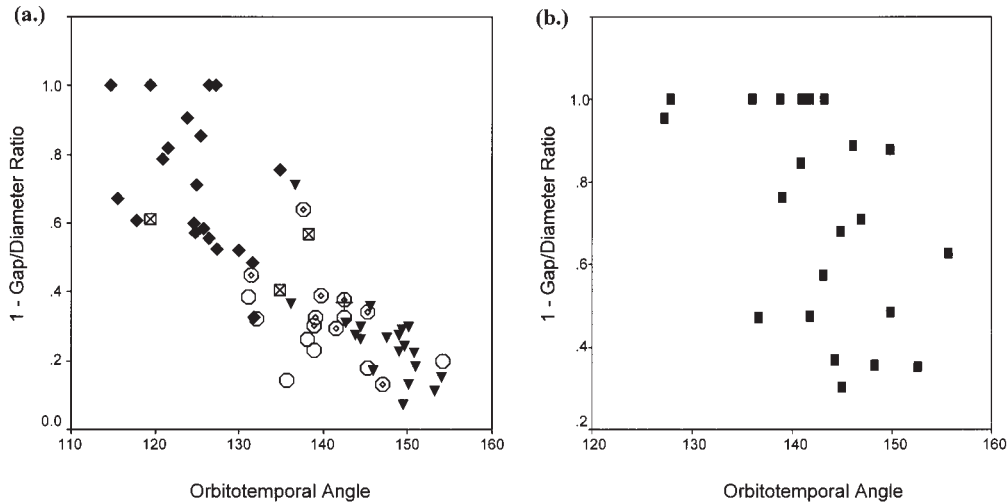


Fig. 10. Relationship between orbitotemporal angle and the ratio of postorbital gap size and orbit diameter in carnivorans. Orbitotemporal angle is plotted in degrees. **a:** The sizes of the postorbital processes are highly negatively correlated with angle between the orbit and the temporal plane in most carnivorans (Spearman's $\rho = -0.848$, $P < 0.001$, $n = 61$). **b:** The distribution of taxa is shifted to higher orbitotemporal angle values in herpestids carnivorans (Spearman's $\rho = -0.535$, $P < 0.001$, $n = 23$). \odot , Canidae; \blacklozenge , Felidae; \blacksquare , Herpestidae; \boxtimes , Hyaenidae; $+$, Nandiniidae; \circ , Procyonidae; \blacktriangledown , Viverridae.

pare between these perissodactyl taxa. Suiform artiodactyls (taxa with processes) have significantly higher orbitotemporal angles than neoselenodont artiodactyls (taxa with bars) (Mann Whitney $U = 13$, $P = 0.001$, $n = 91$).

Orbit and braincase size. Relative orbit diameter and relative braincase size have both been suggested to covary with orbit orientation and postorbital process size. As demonstrated above, orbit diameter and variables of relative braincase size are correlated with orbitotemporal angle, which has been shown to be related to postorbital process size. The following analyses were conducted in order to determine whether relative orbit diameter and braincase size are correlated with the gap-diameter ratio when variance in orbitotemporal angle is held constant. Partial correlation analyses are restricted to the "All Taxa," carnivoran, chiropteran, and artiodactyl datasets, which are those that show significant patterns of correlations among the pertinent variables.

Across all taxa, relative orbit diameter is not correlated with gap-diameter ratio (Table 2: All Taxa). Gap-diameter ratio is negatively correlated with relative braincase length when orbitotemporal angle is held constant (partial correlation coefficient = -0.141 , $P < 0.01$, $n = 330$). Among chiropterans, relative orbit diameter and relative braincase length are uncorrelated with gap-diameter ratio when orbitotemporal angle is held constant. Among carnivorans (excluding herpestids), relative orbit diameter and relative braincase volume are both correlated with gap-diameter ratio when orbitotemporal angle is held constant (orbit diameter, partial correlation coefficient = -0.453 , $P < 0.001$, $n = 330$; relative braincase volume [cube root] partial corre-

lation coefficient = -0.263 , $P < 0.05$, $n = 329$). Among artiodactyls, both orbit diameter and relative braincase volume are both correlated with gap-diameter ratio when orbitotemporal angle is held constant (relative orbit diameter, partial correlation coefficient = 0.587 , $P < 0.001$, $n = 20$; relative braincase volume [cube root] partial correlation coefficient = -0.746 , $P < 0.01$, $n = 20$). It should be noted that orbit diameter and braincase volume are highly correlated in artiodactyls. Relative braincase volume is also correlated with gap-diameter ratio when both orbitotemporal angle and orbit diameter are held constant (partial correlation coefficient = -0.573 , $P < 0.01$, $n = 19$).

DISCUSSION

Orbitotemporal Variation and Postorbital Bar Evolution

The first prediction of the hypothesis being tested is that a decrease in the orbitotemporal angle is correlated with replacement of the postorbital ligament by bone. This prediction is corroborated by the morphometric data analyzed in this study. Across and within groups of mammals, with one important exception, orbitotemporal angle and the gap-diameter ratio were correlated. Metatherians deviate from this general relationship. One explanation for this may be that the metatherians included in this study do not vary much in either orbitotemporal angle or gap-diameter ratio. It is possible that this is true of metatherians in general. Neither of the marsupials to evolve postorbital bars, *Thylacosmilus* or *Thylacoleo*, were available and therefore were not included in this study. So it is not clear whether

these two taxa differ significantly from other metatherians in orbitotemporal angle.

Among groups that do display variance in these variables, the general relationship is demonstrated. Taxa with nearly coplanar orbits and temporal fossae have large postorbital ligaments, and those with orbits that deviate at an angle from the temporal fossae have larger postorbital processes and smaller ligaments. The evolution of postorbital bars in taxa with low orbitotemporal angles is suggested primarily by the results of the megachiropteran and carnivoran analyses. These are the two groups that span the range of lateral orbital wall morphology and orbitotemporal angle, and both contain taxa that are polymorphic for processes and bars. Both groups show highly significant correlations between orbitotemporal angle and gap-diameter ratio. It is noteworthy that carnivorans have two overlapping distributions. Herpestids display a "grade shift" relative to all other carnivorans; these taxa form large processes and complete postorbital bars at higher orbitotemporal angles compared to other carnivorans. It is noteworthy that herpestid carnivorans have less tolerance for binocular image disparity than feliform carnivorans (Packwood and Gordon, 1975; Moran et al., 1983; see Heesy et al., 2005), meaning that less image disparity is required to induce diplopia in, for example, *Suricata* than in *Felis*. In this regard, herpestids are more similar to anthropoids in their disparity tolerance than to other mammals, including other carnivorans (Heesy et al., 2005). It is reasonable to suggest that herpestids form large postorbital processes and complete bars at higher orbitotemporal angles than other carnivorans because they require more stable lateral orbits at comparable orbitotemporal angles. Nevertheless, for both carnivorans and megachiropterans, the taxa (or individuals in polymorphic species) with the lowest orbitotemporal values for each of these groups are those with complete bars. In other words, those megachiropterans or carnivorans in which the orbits tend to deviate most from the temporal fossa are also those that tend to possess complete postorbital bars. This also suggests that, just as there are two distributions within carnivorans, each with a relationship that is specific between orbitotemporal angle and gap-diameter ratio, the angle at which postorbital bars form may be taxon-specific. For example, the range in orbitotemporal angle for *Equus* (taxa with bars) is 128–135°, whereas in the most closely related taxa in this study, species of *Tapirus* (which do not have bars) it is 147–155°. Similarly, suiform artiodactyls (taxa with postorbital ligaments) range from 139–157°, whereas neoselenodonts (taxa with bars) range from 109–138° (with the notable exception of the outlier, *Hyemoschus aquaticus*). Neoselenodont artiodactyls and equines possess bars at orbitotemporal angles more similar to herpestids than to other carnivorans, which tend to range lower in orbitotemporal angle.

One explanation for the differences between taxa in the ranges at which they form complete bars is that relative eye size explains some variance in postorbital ossification (Fig. 2; Heesy, 2003; see also Cartmill, 1972, 1980). Taxa with relatively large eye sizes for their body size tend to have more ossified lateral orbits. Although eye dimensions were not available for the comparative sample analyzed here, it is reasonable to suggest that variance in postorbital process size due to eye size is additive, with the variance explained by orbitotemporal angle. In addition, it is also important to note that the results of the partial correlation analyses of orbitotemporal angle indicate that the effects of relative orbit size and braincase size differentially reorient the orbitotemporal region. For example, the effects of these variables are opposite in nonherpestid carnivorans and megachiropterans. Therefore, these variables likely contribute to the differences in thresholds for the elimination of the postorbital gaps among various groups of mammals.

Another important result is the finding that mammalian taxa with incomplete lateral orbits all have orbitotemporal angles values greater than 114°. The taxa with lower (and the lowest) orbitotemporal angles are predominantly haplorhine primates (i.e., *Tarsius* and anthropoids). This result is especially interesting because this group is unique among mammals in possessing a bony structure known as the postorbital septum (e.g., Cartmill, 1980), which, with the postorbital bar, largely walls off the orbit from the temporal fossa. These taxa, especially anthropoids, have orbits that are among the most convergent, frontated, and closest to vertical among mammals. It has been hypothesized that due to the derived orbit orientation in this group, the anterior temporalis muscle is rostrally displaced, necessitating the postorbital septum to insulate the eye from its actions during mastication (Cartmill, 1980; Ross 1995a,b, 1996, 2000; Ross and Hylander, 1996, 2000). Relating this back to the general pattern of orbit orientation and morphology observed in other mammals, perhaps the 100–110° orbitotemporal angle represents a morphological lower bound beyond which major structural reorganization of the skull is required to maintain the functional integrity of both the visual and masticatory systems. Haplorhines, with their virtually unique orbit orientation among mammals, represent a radical departure from other mammals.

Most variation in orbitotemporal angle is due to orbit orientation when evaluated in the context of the morphological variables examined in this study. Orbit frontation explains most of the variance in orbitotemporal angle. This is so not only when all taxa are considered together, but also for the analyses within orders. Orbitotemporal angle is consistently most highly correlated with frontation among orbit orientation variables when groups are analyzed individually (Table 2). This suggests that this

one particular type of orbit reorientation tends to lead to deviation of the orbit away from the temporal fossa more consistently than convergence and verticality, although these latter two variables are important among many taxa. That the variance explained in orbitotemporal angle by frontation differs from that explained by verticality may be due to the fact that frontation measures the orientation of the orbit relative to the braincase, which is intimately associated with the temporal fossa. In other words, reorienting the orbit relative to the braincase nearly synchronously reorients it relative to the temporal fossa.

The results of this study can shed light on those of previous studies. Previous work found that convergence and frontation were differentially correlated with the occurrence of postorbital bars in megachiropterans, and herpestid and felid carnivorans (Noble et al., 2000; Ravosa et al., 2000a). These patterns of correlations in megachiropterans and carnivorans are explained by the fact that these measures of orbit orientation, in addition to verticality, are correlated with orbitotemporal angle, the measure of the orientation of the orbit relative to the temporal fossa. It was not clear in these previous studies why some taxa had bars at intermediate levels of frontation or convergence. It is reasonable to suggest that it is because these taxa had low orbitotemporal angles due to the cumulative variance explained by all measures of orbit orientation, as well as in some cases variance added due to orbit size. Orbitotemporal angle variation and postorbital bar evolution are not only associated in these taxa, but across mammals. However, the results of this study do not agree with the suggestion that increasing encephalization (assumed in this study to be relative cube root of braincase volume or relative braincase length) is the cause of increases in frontation (Noble et al., 2000; Ravosa et al., 2000a), and, by association, with the formation of postorbital bars. In chiropterans and artiodactyls, relative braincase volume is negatively correlated with orbitotemporal angle, which is interpreted as the orbit and temporal fossa deviating more with increasing braincase volume. However, primates and carnivorans show the opposite pattern: increasing relative braincase size leads to a larger orbitotemporal angle, or less deviation between the orbit and temporal fossa. These data may be viewed as contradictory to previous studies (Noble et al., 2000; Ravosa et al., 2000a). It is not clear that these data are directly comparable because the measures of orbitotemporal angle and external braincase volume are unique to this study. It is reasonable to hypothesize that the correlates of orbit orientation are multifactorial, with adaptively different taxa reorienting their orbits for various reasons (Cartmill, 1972, 1974; Ross, 1995a, 1996; Heesy, 2003). Taxa with bars have dissimilar orbit orientations, but they are united by similar relationships between the orbit and temporal fossa.

Based on the results of this study, it can be concluded that Cartmill's (1970, 1972, 1980) hypothesis was essentially correct: reorientation of the orbit relative to the temporal fossa is correlated with the sizes of postorbital processes in taxa with relatively large eye sizes. One factor that was not identified by Cartmill was orbit frontation, which was found by Ravosa and colleagues (Noble et al., 2000; Ravosa et al., 2000a) also to be associated with evolution of bars in megachiropterans, and herpestid and felid carnivorans. The results of this study show that the importance of convergence, frontation, and verticality to orbitotemporal angle differ among taxa. Nevertheless, reorientation of the orbit is the primary influence on orbitotemporal angle and morphology.

Cartmill (1970) limited his explanation of bar evolution to small-sized taxa, and left open the possibility that another explanation applied to bar evolution in ungulates. The results of this study show that neoselenodonts and equines are similar to other taxa with bars in the orientation of the orbitotemporal region. Orbit reorientation of a different form is a factor in ungulates. Cartmill may have identified a generalized morphological construction rule for mammals. The evolution of processes and bars in mammals is governed by the same causal mechanism and follows the same morphological transformation series. This is demonstrated by several independent replications of bars as well as multiple instances of the evolution of processes, all of which fit a generalized pattern in mammals.

Function of the Mammalian Postorbital Bar

As demonstrated in the previous section, taxa with orbits that deviate substantially from the plane of the temporal fossa have bony lateral orbital margins. This morphological configuration unites the groups that have independently evolved postorbital bars (primates, neoselenodont artiodactyls, equine perissodactyls, and scandentians), as well as those taxa among megachiropterans and carnivorans for which bars are a polymorphic trait. In these taxa, the postorbital ligament has been replaced by bone to stiffen the lateral orbit and prevent deformation during mastication. It has been suggested that this is to maintain oculomotor stability (Collins, 1921; Cartmill, 1970, 1972, 1980; see also Ravosa et al., 2000b). The need for a stable lateral orbital margin is related to the anatomy of the orbit and normal oculomotor control.

There are several components of orbital anatomy that are crucial for maintaining eye position and oculomotor stability in mammals. Principal among these are the ligamentous attachments that suspend the eye within the orbit and maintain the normal or rest position. In humans, connective tissue extends from Tenon's capsule (the fibrous membrane that envelops the eye from the cornea to the optic nerve) to the periorbita (Wolff, 1948; Koornneef, 1992). The

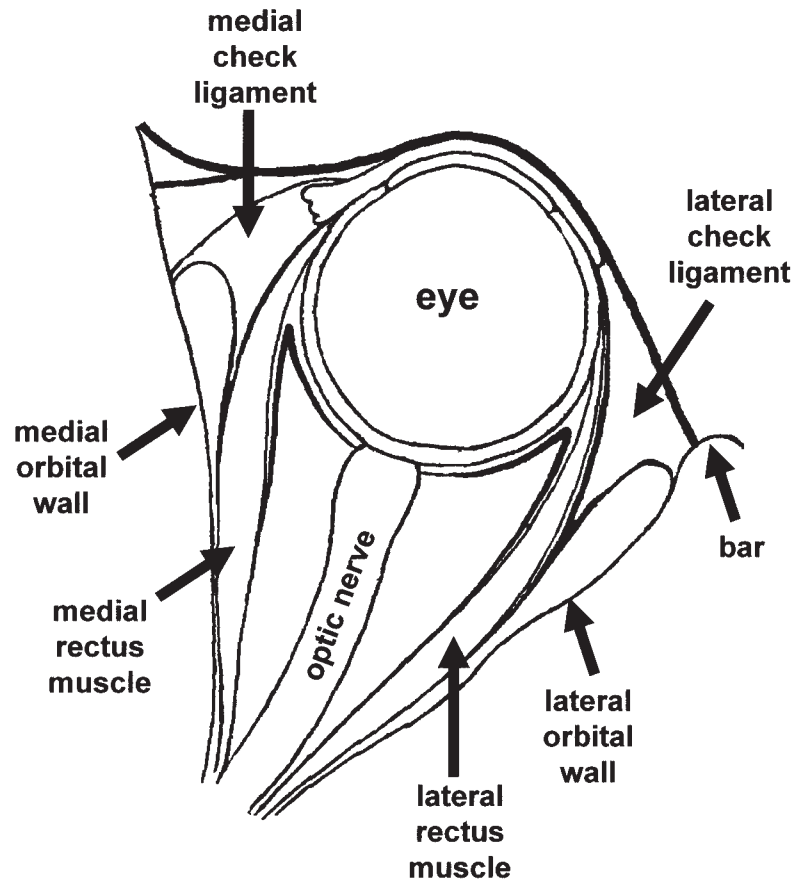


Fig. 11. Schematic anatomy of the human orbit in transverse cross-section. (Figure redrawn and schematized from Bannister et al., 1995.)

check ligaments of the medial and lateral recti, which attach to the medial and lateral palpebral ligaments as well as the lacrimal and lateral orbital rim, respectively, in humans, have long been thought to be collagenous extensions of the recti (Lockwood, 1886; Bannister et al., 1995; see Fig. 11). Recent work has demonstrated that not only do these “check ligaments” contain innervated muscular components but that these, in synergism with the so-called orbital heads of the extraocular muscles, function as specialized pulleys of the extraocular muscles, and have been found in humans, macaques, rabbits, and rats (e.g., Demer et al., 1995, 1997; Clark et al., 1997, 1998; Khanna and Porter, 2001; Briggs and Schachat, 2002). The medial and lateral extraocular muscle pulleys are believed to function to maintain linear position of the eye and influence the position of its rotational axis (Demer et al., 2000; Demer, 2002; Haslwanter, 2002). The orbital heads may also contribute to eye movement during saccadic (foveating) movements (Briggs and Schachat, 2002; Demer, 2002).

Displacement of these extraocular muscle pulleys in humans due to abnormal development, surgery, or orbital “blow out” fractures causes misalignment and improper rotation, and is associated with strabismus, the deviation of the visual axis of the affected eye during normal vision (Koornneef, 1992;

Miller and Demer, 1992; Clark et al., 1998; Abramoff et al., 2002). The lateral pulley in particular is important when considering the functional implications of Cartmill’s model. In rats and rabbits, the pulley of the lateral rectus attaches to the postorbital ligament, whereas in macaques and humans it attaches to the lateral orbital rim (Eglitis, 1964; Demer et al., 2000; Khanna and Porter, 2001). In the type of orbit deformation described by Cartmill, contraction of the anterior temporalis muscle and tension in the temporalis fascia (of which the postorbital ligament is the anteriormost portion) would deform the postorbital ligament and also displace the pulleys of the lateral and superior recti. Displacement and the associated change in tension of the pulleys during mastication would probably cause symptoms similar to those experienced by humans with congenital oculomotor dysfunction or injuries to the lateral orbital wall. There are numerous neural circuits responsible for maintaining eye position that depend on a stable orbit because corrective eye movements are made by the extraocular muscles, which require predictable orbit position (Heesy et al., 2005). If the orbit were deformed during such corrective contractions of the extraocular muscles, then the subsequent eye movements would cause misalignment. In other words, the function of the postorbital bar is to maintain a stiff lateral orbit

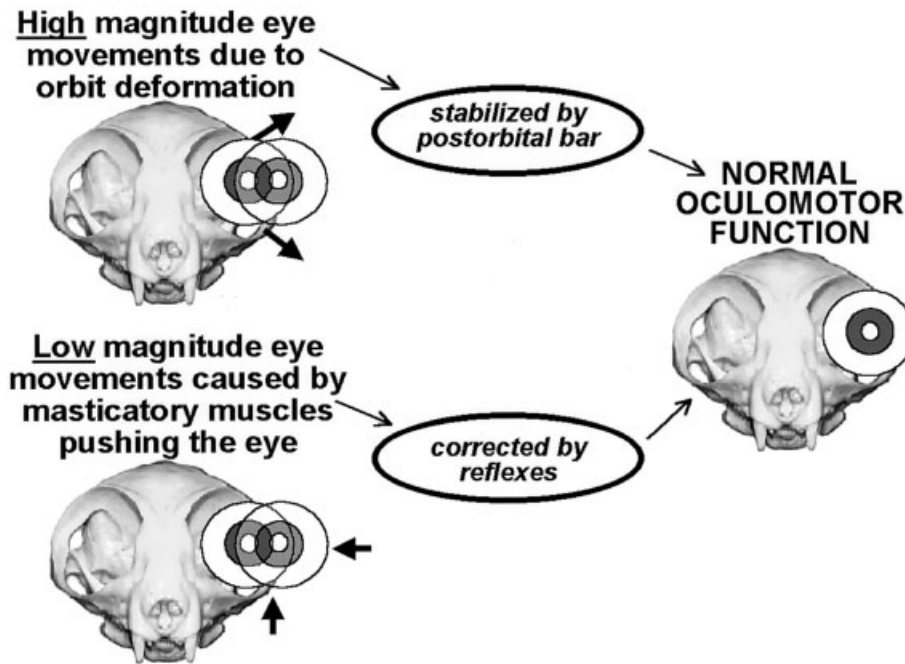


Fig. 12. Model of the function of the mammalian postorbital bar. The function of the postorbital bar is to maintain a stiff lateral orbit to prevent gross deformation of the orbital margin, which prevents large magnitude eye movements that would otherwise be caused by deformation of the orbit. A stable orbit provides substrate from which the extraocular muscle system can compensate for the remaining small-scale eye movements that are caused by contraction of the anterior temporalis and medial pterygoid.

to prevent gross deformation of the orbital margin (illustrated in Fig. 12). This achieves two things. First, as suggested by Cartmill (1970, 1972), the postorbital bar ameliorates gross eye movements caused by deformation of the orbit. Second, it provides a stable substrate from which the extraocular muscle system can compensate for the remaining small-scale eye movements that are caused by contraction of the anterior temporalis and medial pterygoid (e.g., Murakami and Cavanagh, 1998, 2001; Heesy, 2003; Heesy et al., 2005). There are several potential behavioral and ecological consequences of visual disruption. While the animal was chewing, accurate location of potential predators or prey would be impossible, and likely the time both during and slightly after chewing would be one of visual confusion, as it is in humans that experience double vision and visual axis misalignment (Heesy et al., 2005). An arboreal animal would be unable to safely move in its environment. For taxa like perissodactyls and artiodactyls, with panoramic visual fields for which a large component of the day is spent masticating, visual axis misalignment due to impingement by the masticatory muscles (a phenomenon known as oscillopsia) would make the visual location of predators difficult. Presumably, the loss of depth perception would not be critical because the visual zone in which depth is perceived (also known as the stereoscopic field) is not large in these taxa (e.g., Hughes, 1977; Hughes and Whitteridge, 1973; Pettigrew et al., 1984), although the stereoscopic portion of the visual field may be critical to taxa that locomote on cliffs and other precarious substrates (Ramachandran et al., 1977).

SUMMARY AND CONCLUSIONS

1) Orbitotemporal angle is correlated with size of postorbital processes. The more the plane of the orbit deviates from the plane of the temporal fossa, the larger the postorbital processes and smaller the postorbital gap (a surrogate for the length of the postorbital ligament). Taxa with complete postorbital bars are those with the lowest orbitotemporal angles for their taxonomic groups.

2) Reorientation of the orbit is the primary influence on orbitotemporal angle. Orbit frontation (the vertical orientation of the orbit relative to the long axis of the braincase) explains most of the variance in orbitotemporal angle, followed by convergence (the degree to which the orbits face in the same direction), and verticality (vertical orientation of the orbit relative to the palate). The importance of each of these types of orbit orientation to orbitotemporal angle differs among taxa. Relative braincase size and relative orbit size influence orbit orientation and, as a result, orbitotemporal angle.

3) The function of the postorbital bar is to stiffen the lateral orbital wall. Muscle pulleys responsible for coordinative and corrective eye movements, as well as ligaments and other connective tissue, attach to the lateral orbital wall including the bar. Without a stiff lateral orbit, deformation due to temporalis contraction would also displace these soft tissues that contribute to normal oculomotor function (Fig. 12).

ACKNOWLEDGMENTS

This work was conducted as a component of my dissertation research. I would like to thank my com-

mittee, Brigitte Demes, Callum Ross, Jack Stern, and Matt Cartmill for assistance. I am grateful for the comments and corrections offered by Steve Frost, Meg Hall, Frederick Harrison, and an especially careful anonymous reviewer to whom, I hope, more of my manuscripts are sent in the future. Jean Spence and Robert Randall facilitated access to the mammalogy collections of the AMNH. Linda Gordon facilitated access to the Smithsonian collections.

LITERATURE CITED

- Abramoff MD, Kalmann R, de Graaf MEL, Stilma JS, Mourits MP. 2002. Rectus extraocular muscle paths and decompression surgery for Graves orbitopathy: mechanism of motility disturbances. *Invest Ophthalmol Vis Sci* 43:300–307.
- Bannister LW, Berry MM, Collins P, Dyson M, Dussek JE, Ferguson MWJ, editors. 1995. *Gray's anatomy: the anatomical basis of medicine and surgery*, 38th ed. Edinburgh: Churchill Livingstone.
- Bininda-Emonds ORP, Gittleman JL, Purvis A. 1999. Building large trees by combining phylogenetic information: a complete phylogeny of the extant Carnivora (Mammalia). *Biol Rev* 74:143–175.
- Briggs MM, Schachat F. 2002. The superfast extraocular myosin (MYH13) is localized to the innervation zone in both the global and orbital layers of rabbit extraocular muscle. *J Exp Biol* 205:3133–3142.
- Cartmill M. 1970. The orbits of arboreal mammals: a reassessment of the arboreal theory of primate evolution. Ph.D. dissertation. Chicago, IL: University of Chicago.
- Cartmill M. 1972. Arboreal adaptations and the origin of the Order Primates. In: Tuttle R, editor. *The functional and evolutionary biology of primates*. Chicago: Aldine. p 97–122.
- Cartmill M. 1974. Rethinking primate origins. *Science* 184:436–443.
- Cartmill M. 1980. Morphology, function, and evolution of the anthropoid postorbital septum. In: Ciochon RL, Chiarelli AB, editors. *Evolutionary biology of the New World monkeys and continental drift*. New York: Plenum. p 243–274.
- Clark RA, Miller JM, Demer JL. 1997. Location and stability of rectus muscle pulleys: muscle paths as a function of gaze. *Invest Ophthalmol Vis Sci* 38:227–240.
- Clark RA, Miller JM, Rosenbaum AL, Demer JL. 1998. Heterotopic muscle pulleys or oblique muscle dysfunction? *JAAPOS* 2:17–25.
- Collins ET. 1921. Changes in the visual organs correlated with the adoption of arboreal life and with the assumption of the erect posture. *Trans Ophthal Soc UK* 41:10–90.
- Corruccini RS. 1995. Of ratios and rationality. *Am J Phys Anthropol* 96:189–191.
- Demer JL. 2002. The orbital pulley system: a revolution in concepts of orbital anatomy. *Ann N Y Acad Sci* 956:17–32.
- Demer JL, Miller JM, Poukens V, Vinters HV, Glasgow BJ. 1995. Evidence for fibromuscular pulleys of the recti extraocular muscles. *Invest Ophthalmol Vis Sci* 36:1125–1136.
- Demer JL, Poukens V, Micevych P. 1997. Innervation of extraocular pulley smooth muscle in monkey and human. *Invest Ophthalmol Vis Sci* 38:1774–1785.
- Demer JL, Oh SY, Poukens V. 2000. Evidence for active control of rectus extraocular muscle pulleys. *Invest Ophthalmol Vis Sci* 41:1280–1290.
- Eglitis I. 1964. The orbital fascia. In: Prince JH, editor. *The rabbit in eye research*. Springfield, IL: Charles C. Thomas. p 28–37.
- Felsenstein J. 1985. Phylogenies and the comparative method. *Am Nat* 125:1–15.
- Fisher NI. 1993. *Statistical analysis of circular data*. New York: Cambridge University Press.
- Greaves WS. 1985. The mammalian postorbital bar as a torsion-resisting helical strut. *J Zool (Lond)* 207:125–136.
- Hair JF, Anderson RE, Tatham RL, Black WC. 1998. *Multivariate data analysis*, 5th ed. Upper Saddle River, NJ: Prentice Hall.
- Hamilton AT, Springer MS. 1999. DNA sequence evidence for placement of the ground cuscus, *Phalanger gymnotis*, in the Tribe Phalangerini (Marsupialia: Phalangeridae). *J Mamm Evol* 6:1–17.
- Haslwanter T. 2002. Mechanics of eye movements: implications of the “orbital revolution.” *Ann N Y Acad Sci* 956:33–41.
- Hassanin A, Douzery EJP. 1999. The tribal radiation of the Family Bovidae (Artiodactyla) and the evolution of the mitochondrial cytochrome *b* gene. *Mol Phylogenet Evol* 13:227–243.
- Hassanin A, Douzery EJP. 2003. Molecular and morphological phylogenies of Ruminantia and the alternative position of the Moschidae. *Syst Biol* 52:206–228.
- Heesy CP. 2003. The evolution of orbit orientation in mammals and the function of the primate postorbital bar. Ph.D. dissertation. Stony Brook, NY: Stony Brook University.
- Heesy CP, Ross CF, Demes B. 2005. Oculomotor stability and the functions of the postorbital bar and septum. In: Ravosa M, Dagosto M, editors. *Primate origins and adaptations*. New York: Kluwer Academic/Plenum.
- Hershkovitz P. 1977. *Living New World monkeys (Platyrrhini)*, vol. 1. Chicago: University of Chicago Press.
- Hiimae K, Jenkins FA. 1969. The anatomy and internal architecture of the muscles of mastication in *Didelphis marsupialis*. *Postilla* 140:1–49.
- Hughes A. 1977. The topography of vision in mammals of contrasting lifestyle: comparative optics and retinal organisation. In: Crescitelli F, editor. *The visual system in vertebrates*. New York: Springer. p 613–756.
- Hughes A, Whitteridge D. 1973. The receptive fields and topographical organization of goat retinal ganglion cells. *Vision Res* 13:1101–1114.
- Hylander WL, Picq PG, Johnson KR. 1991. Masticatory-stress hypotheses and the supraorbital region of primates. *Am J Phys Anthropol* 86:1–36.
- Jones KE, Purvis A, MacLarnon A, Bininda-Emonds ORP, Simmons NB. 2002. A phylogenetic supertree of the bats (Mammalia: Chiroptera). *Biol Rev* 77:223–259.
- Jungers WL, Falsetti AB, Wall CE. 1995. Shape, relative size, and size-adjustments in morphometrics. *Yrbk Phys Anthropol* 38:137–161.
- Khanna S, Porter JD. 2001. Evidence for rectus extraocular muscle pulleys in rodents. *Invest Ophthalmol Vis Sci* 42:1986–1992.
- Kirsch JAW, Bleiweiss RE, Dickerman AW, Reig OA. 1993. DNA/DNA hybridization studies of carnivorous marsupials. III. Relationships among species of *Didelphis* (Didelphidae). *J Mamm Evol* 1:75–97.
- Koornneef L. 1992. Orbital connective tissue. In: Tasma W, editor. *Duane's foundations of clinical ophthalmology*. Philadelphia: J. S. Lippincott. p 1–23.
- Lockwood CA, Lynch JM, Kimbel WH. 2002. Quantifying temporal bone morphology of great apes and humans: an approach using geometric morphometrics. *J Anat* 201:447–464.
- Lockwood CB. 1886. The anatomy of the muscles, ligaments, and fasciae of the orbit, including an account of the Capsule of Tenon, the check ligaments of the recti, and of the suspensory ligament of the eye. *J Anat Physiol* 20:1–25.
- Martins EP. 2001. COMPARE, v. 4.4. Computer programs for the statistical analysis of comparative data. Distributed by the author via the Internet at <http://compare.bio.indiana.edu/>. Department of Biology, Indiana University, Bloomington, IN.
- Martins EP, Hansen TF. 1997. Phylogenies and the comparative method: A general approach to incorporating phylogenetic information into the analysis of interspecific data. *Am Nat* 149:646–667.
- McKenna MC, Bell SK. 1997. *Classification of mammals above the species level*. New York: Columbia University Press.
- Mercer JM, Roth VL. 2003. The effects of Cenozoic global change on squirrel phylogeny. *Science* 299:1568–1572.

- Miller JM, Demer JL. 1992. Biomechanical analysis of strabismus. *Binoc Vis Eye Mus Surg Q* 7:233–248.
- Moran G, Timney B, Sorenson L, Desrochers B. 1983. Binocular depth perception in the Meerkat (*Suricata suricatta*). *Vision Res* 23:965–969.
- Murakami I, Cavanagh P. 1998. A jitter after-effect reveals motion-based stabilization of vision. *Nature* 395:798–801.
- Murakami I, Cavanagh P. 2001. Visual jitter: evidence for a visual-motion-based compensation of retinal slip due to small eye movements. *Vision Res* 41:173–186.
- Noble VE, Kowalski EM, Ravosa MJ. 2000. Orbit orientation and the function of the mammalian postorbital bar. *J Zool (Lond)* 250:405–418.
- Packwood J, Gordon B. 1975. Stereopsis in normal domestic cat, Siamese cat, and cat raised with alternating monocular occlusion. *J Neurophysiol* 38:1485–1499.
- Patton JL, dos Reis SF, da Silva MN. 1996. Relationships among didelphid marsupials based on sequence variation in the mitochondrial cytochrome B gene. *J Mamm Evol* 3:3–29.
- Pettigrew JD, Ramachandran VS, Bravo H. 1984. Some neural connections subserving binocular vision in ungulates. *Brain Behav Evol* 24:65–93.
- Prince JH. 1953. Comparative anatomy of the orbit. *Br J Physiol Optics* 10:144–154.
- Prince JH. 1956. Comparative anatomy of the eye. Springfield, IL: Charles C. Thomas.
- Purvis A. 1995. A composite estimate of primate phylogeny. *Philos Trans R Soc Lond* 348:405–421.
- Purvis A, Webster AJ. 1999. Phylogenetically independent comparisons and primate phylogeny. In: Lee PC, editor. *Comparative primate socioecology*. New York: Cambridge University Press. p 44–70.
- Radinsky LB. 1983. Allometry and reorganization in horse skull proportions. *Science* 221:1189–1191.
- Radinsky LB. 1984. Ontogeny and phylogeny in horse skull evolution. *Evolution* 38:1–15.
- Ramachandran VS, Clarke PGH, Whitteridge D. 1977. Cells selective to binocular disparity in the cortex of newborn lambs. *Nature* 268:333–335.
- Randi E, Lucchini V, Diong CH. 1996. Evolutionary genetics of the Suiformes as reconstructed using mtDNA sequencing. *J Mamm Evol* 3:163–194.
- Ravosa MJ. 1991a. Interspecific perspective on mechanical and nonmechanical models of primate circumorbital morphology. *Am J Phys Anthropol* 86:369–396.
- Ravosa MJ. 1991b. Ontogenetic perspective on mechanical and non-mechanical models of primate circumorbital morphology. *Am J Phys Anthropol* 85:95–112.
- Ravosa MJ, Johnson KR, Hylander WL. 2000a. Strain in the galago facial skull. *J Morphol* 245:51–66.
- Ravosa MJ, Noble VE, Hylander WL, Johnson KR, Kowalski EM. 2000b. Masticatory stress, orbital orientation and the evolution of the primate postorbital bar. *J Hum Evol* 38:667–693.
- Ritland S. 1982. The allometry of the vertebrate eye. Ph.D. dissertation. Chicago, IL: University of Chicago.
- Rohlf FJ. 2001. Comparative methods for the analysis of continuous variables: geometric interpretations. *Evolution* 55:2143–2160.
- Ross CF. 1995a. Allometric and functional influences on primate orbit orientation and the origins of the Anthropoidea. *J Hum Evol* 29:201–227.
- Ross CF. 1995b. Muscular and osseous anatomy of the primate anterior temporal fossa and the functions of the postorbital septum. *Am J Phys Anthropol* 98:275–306.
- Ross C. 1996. Adaptive explanation for the origins of the Anthropoidea (Primates). *Am J Primatol* 40:205–230.
- Ross CF. 2000. Into the light: the origin of Anthropoidea. *Annu Rev Anthropol* 29:147–194.
- Ross CF. 2001. In vivo function of the craniofacial haft: the interorbital “pillar.” *Am J Phys Anthropol* 116:108–139.
- Ross CF, Hylander WL. 1996. In vivo and in vitro bone strain in the owl monkey circumorbital region and the function of the postorbital septum. *Am J Phys Anthropol* 101:183–215.
- Ross C, Hylander WL. 2000. Electromyography of the anterior temporalis and masseter muscles of owl monkeys (*Aotus trivirgatus*) and the function of the postorbital septum. *Am J Phys Anthropol* 112:455–468.
- Ross CF, Ravosa M. 1993. Basicranial flexion, relative brain size and facial kyphosis in nonhuman primates. *Am J Phys Anthropol* 91:305–324.
- Ross CF, Henneberg M, Ravosa MJ, Richard S. 2004. Curvilinear, geometric and phylogenetic modeling of basicranial flexion: is it adaptive, is it constrained? *J Hum Evol* 46:185–213.
- Ross CF, Hall MI, Heesy CP. 2005. Were basal primates nocturnal? Evidence from eye and orbit shape. In: Ravosa M, Dagosto M, editors. *Primate origins and adaptations*. New York: Kluwer Academic/Plenum.
- Simons EL. 1962. Fossil evidence relating to the early evolution of primate behavior. *Ann N Y Acad Sci* 102:282–294.
- Sokal RR, Rohlf FJ. 1995. *Biometry*, 3rd ed. New York: W.H. Freeman.
- Springer MS, Westerman M, Kirsch JAW. 1994. Relationships among orders and families of marsupials based on 12S ribosomal DNA sequences and the timing of the marsupial radiation. *J Mamm Evol* 2:85–115.
- Wolff E. 1948. *The anatomy of the eye and orbit*, 3rd ed. Philadelphia: Blakiston.
- Yoder AD, Burns MM, Zehr S, Delefosse T, Veron G, Goodman SM, Flynn JJ. 2003. Single origin of Malagasy Carnivora from an African ancestor. *Nature* 421:734–737.